International Geology Review
Publication details, including instructions for authors and subscription information:
http://www.tandfonline.com/loi/tigr20

K-Ar Dating, Geochemical, and Sr-Nd-Pb Isotopic Systematics of Late Mesozoic Mafic Dikes, Southern Jiangxi Province, Southeast China: Petrogenesis and Tectonic Implications

Guiqing Xie [a], Ruizhong Hu [b], Jingwen Mao [c], Franco Pirajno [d], Ruiling Li [b], Jinjian Cao [b], Guohao Jiang [b] & Junhong Zhao [b]

[a] China University of Geosciences

[b] Institute of Geochemistry, Chinese Academy of Sciences

[c] Institute of Mineral Resources, Chinese Academy of Geological Sciences

[d] Geological Survey of Western Australia

Published online: 16 Jul 2010.

To cite this article: Guiqing Xie , Ruizhong Hu , Jingwen Mao , Franco Pirajno , Ruiling Li , Jinjian Cao , Guohao Jiang & Junhong Zhao (2006): K-Ar Dating, Geochemical, and Sr-Nd-Pb Isotopic Systematics of Late Mesozoic Mafic Dikes, Southern Jiangxi Province, Southeast China: Petrogenesis and Tectonic Implications, International Geology Review, 48:11, 1023-1051

To link to this article: http://dx.doi.org/10.2747/0020-6814.48.11.1023

International Geology Review, Vol. 48, 2006, p. 1023–1051.

K-Ar Dating, Geochemical, and Sr-Nd-Pb Isotopic Systematics of Late Mesozoic Mafic Dikes, Southern Jiangxi Province, Southeast China: Petrogenesis and Tectonic Implications

GUIQING XIE,[1]

State Key Laboratory of Geological Processes and Mineral Resources, China University of Geosciences, Beijing, 100083, China; Institute of Mineral Resources, Chinese Academy of Geological Sciences, Beijing, 100037, China; and Key Laboratory of Ore Deposit Geochemistry, Institute of Geochemistry, Chinese Academy of Sciences, Guiyang, 550002, China

RUIZHONG HU,

Key Laboratory of Ore Deposit Geochemistry, Institute of Geochemistry, Chinese Academy of Sciences, Guiyang, 550002, China

JINGWEN MAO,

Institute of Mineral Resources, Chinese Academy of Geological Sciences, Beijing, 100037, China

FRANCO PIRAJNO,

Geological Survey of Western Australia, 100 Plain Street, Perth, WA 6004, Australia

RUILING LI, JINJIAN CAO, GUOHAO JIANG, AND JUNHONG ZHAO

Key Laboratory of Ore Deposit Geochemistry, Institute of Geochemistry, Chinese Academy of Sciences, Guiyang, 550002, China

Abstract

A geochemical and isotopic study was carried out on late Mesozoic mafic dikes in southern Jiangxi Province in order to clarify their petrogenesis and explore tectonic implications. K-Ar dating results show that these mafic dikes intruded during Jurassic to Late Cretaceous (147–79 Ma) time. Dominantly sub-alkaline in composition, these dikes share several geochemical features: they are significantly enriched in large-ion lithophile element (LILE, e.g., Rb, Ba, Sr) and slightly enriched in light rare-earth elements (LREE), and are variably depleted in high-field-strength elements (HFSE, e. g., Nb, Ta, Ti). However, mafic dikes intruded in the Late Jurassic to Early Cretaceous (147–139 Ma) are also characterized by weaker Nb and Ta negative anomalies compared with dikes intruded in the mid-Late Cretaceous (118–78 Ma). Age-corrected Sr-Nd isotopic ratios show relatively wide ranges for $(^{87}Sr/^{86}Sr)_i$ from 0.7042 to 0.7130 , and –10.8 to +5.9 for $\varepsilon_{Nd}(T)$. $^{206}Pb/^{204}Pb$, $^{207}Pb/^{204}Pb$, and $^{208}Pb/^{204}Pb$ ratios for these dikes range from 17.819 to 18.400, 15.472 to 15.730, and 37.711 to 38.787, respectively. Geological, geochemical, and isotopic evidence suggests that the mafic dikes in southern Jiangxi Province were not significantly affected by crustal contamination. We consider them to have originated from dominantly EM-2 type lithospheric mantle ± minor asthenospheric mantle (MORB or DMM). The geochemical and Sr-Nd-Pb isotopic characteristics of basalts and mafic dikes, together with geochemical and isotopic data from granitoids, volcanic rocks, and rift basins in Southeast China suggest that this region was dominated by a lithospheric extensional tectonic regime in the late Mesozoic. This study, integrated with published geochemical and isotopic data for upper Mesozoic and Cenozoic basaltic rocks, allows us to postulate that lithospheric thinning in Southeast China continued until the end of Late Cretaceous time, and was accompanied by a shift in the mantle sources of basaltic rocks.

Introduction

THE SOUTHEASTERN MARGIN of Eurasia is characterized by widespread Mesozoic igneous provinces in which granitoids and rhyolites are volumetrically dominant, with minor basaltic rocks (Zhou and Li, 2000). Cenozoic basalts are the chief volcanic rocks and are widely distributed along the coastal region in Southeast China (e.g., Zou et al., 2000; Ho et al., 2003). It is generally accepted that Late Cenozoic volcanism was related to lithospheric extension due to asthenospheric upwelling (Chung et al., 1994,

[1]Corresponding author; email: guiqingxie@sohu.com

1995; Qi et al., 1994; Zou et al., 2000; Ho et al., 2003). However, the tectonic regime that accounts for Mesozoic magmatism in Southeast China has been a contentious issue for the last two decades. Two tectonic models have recently been advocated. In the first, the tectonic setting for Southeast China's magmatism is related to paleo-Pacific subduction, which prevailed until the Late Cretaceous (e.g., Jahn et al., 1990; Lapierre et al., 1997; Zhou and Li, 2000). In the second, this magmatism is related to continental extension, which was dominant in Southeast China during the Jurassic and Cretaceous periods (e.g., Gilder et al., 1991, 1996; Li, 2000; Ren et al., 2002). The tectonic setting can be compared to that of the Lachlan orogen of eastern Australia (Collins, 2002). These types of orogens are characterized by what Collins (2002) called "extensional accretionary orogens," in which backarc extension, due to subducting slab retreat, causes asthenospheric upwelling, crustal melting, formation of rift basins, emplacement of granitic rocks and eruption of basaltic rocks. Granite isotopic characteristics as well as the presence of possible metamorphic core complexes suggest that lithospheric extension in Southeast China occurred concomitantly with paleo-Pacific subduction (Gilder et al., 1991, 1996) and that Mesozoic extensional tectonics, within a subduction system, did occur in this region (Faure et al., 1996). Therefore, Southeast China provides a good opportunity to study the changing nature of the mantle source in an extensional tectonic regime within a subduction system. In addition, until recently, the regional nature of the Mesozoic mantle beneath the crust remained unclear.

Studies of mantle-derived xenoliths, integrated with seismic and geothermal data, indicate that an ancient lithospheric mantle, up to 200 km thick, was removed and replaced by new asthenospheric material and that lithospheric thinning occurred during late Mesozoic to Cenozoic time (Hu et al., 2000; Xu et al., 2000; Yang, 2003). Nevertheless, the timing and mechanisms for lithospheric thinning remain poorly understood, largely owing to the lack of knowledge about the nature of the Mesozoic mantle source in this region (Zheng et al., 2004).

Mesozoic mafic dikes are widespread and spatially associated with igneous rocks in Southeast China (e.g., Li and McCulloch, 1998). These mafic dikes of variable ages can give insights into the changing nature of the mantle source in this region. However, their systematic geochemical and isotopic compositions are poorly known (Lan et al., 1995; Li and McCulloch, 1998; Zhao et al., 2004). Available regional geological surveys in Southeast China show that Mesozoic mafic dikes are most common in southern Jiangxi Province and adjacent regions (Zhou, 2003). In this paper, we present new K-Ar results, geochemical and Nd-Sr-Pb isotopic data for the mafic dikes in southern Jiangxi Province. The results of this work are used to document the geochemical and isotopic characteristics of the dikes, and discuss their petrogenesis, mantle source, and tectonic implications. In addition, our data integrated with published geochemical and isotopic systematics of late Mesozoic and Cenozoic basaltic magmatism elsewhere in Southeast China allows us to discuss implications for regional lithospheric thinning beneath the crust.

Geological Setting

Southeast China comprises two tectonic blocks, separated by the Jianshan-Shaoxing fault (Zhang et al., 2005), the Cathaysian block in the southeast, and the Yangtze block in the northwest. These blocks were amalgamated during the Jinning orogenic event in the Neoproterozoic (about 970 Ma) (e.g., Li and McCulloch, 1996). The Cathaysian block may be divided into a western and eastern Cathaysian blocks by the Guangchang-Xunwu fault zone, which is a translithospheric discontinuity reflected in Bouguer gravity anomalies and seismic tomography (Li et al., 2001; Fig.1). The Cathaysian block has a complex tectono-magmatic history, which was developed on a Precambrian (Paleoproterozoic to Mesoproterozoic, and possibly late Archean) basement that is composed of greenschist- and amphibolites-facies metamorphic rocks (Chen and Jahn, 1998; Xu et al., 2005). The Precambrian basement is overlain uncomformably by Paleozoic sedimentary rocks. From Jurassic to Cretaceous time, Southeast China was affected by intensive magmatic activity, which included volumetrically dominant granites and rhyolites, with subordinate gabbros and basalts, and rare intermediate rocks (Zhou and Li, 2000). Whether a continuous extensional setting characterized the tectonics of Southeast China throughout the Mesozoic is still open to question. Nevertheless, recent studies indicate that the Cathaysia block was subjected mainly to an extensional tectonic regime during the Mesozoic (Zhou and Li, 2000; Li, 2000; Li et al., 2003, 2004; Xing et al., 2004). This extensional regime may have resulted in the formation of Late Cretaceous to Early Tertiary pull-apart basins

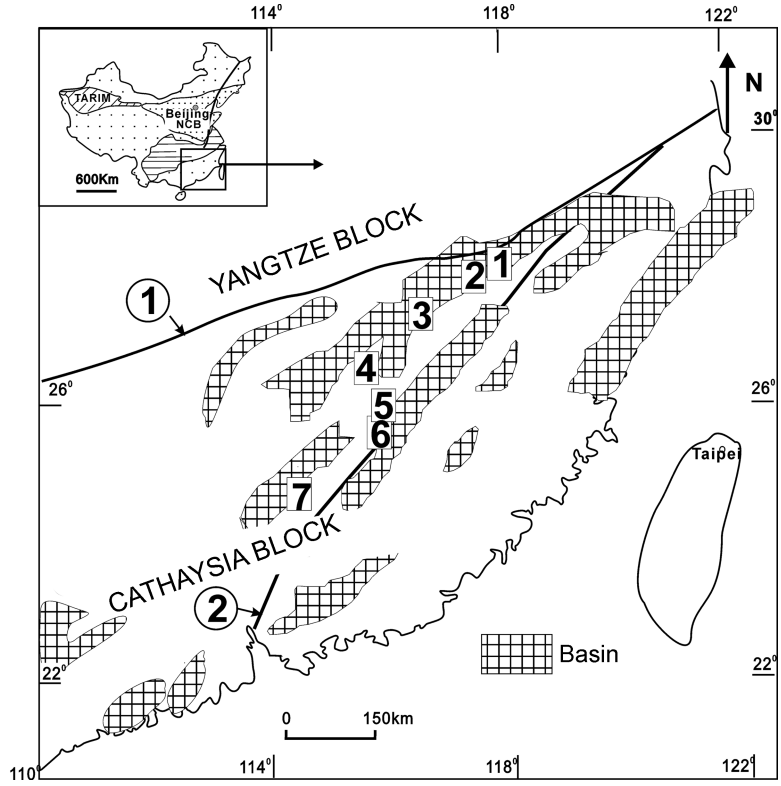

FIG. 1. Simplified geological map of southern Jiangxi Province, Southeast China, showing sample localities for this study (modified after Gilder et al., 1991). Numbered circles: 1 = Jiangshan-Shaoxing fault zone; 2 = Guangchang-Xunwu fault zone. Location of mafic dikes discussed in the text (numbers): 1 = Wuyishan; 2 = Danyan; 3 = Maopai; 4 = Shandai; 5 = Caotaobei; 6 = Yanbei; 7 = Daijishan. Abbreviations: NCB = North China block.

and subsidence of the Taiwan Strait accompanied by the opening of the South China Ocean (Chung et al., 1997; Zhu et al., 2004). Meanwhile, Late Cenozoic intra-plate basalts were erupted in these basins, with some carrying abundant mantle-derived xenoliths (e.g., Qi et al., 1995; Xu et al., 2000, 2002, 2003; Wang and O'Reilly, 2003).

Southern Jiangxi Province is located in the eastern part of the West Cathaysian block and along the southeastern boundary of the Yangtze block (Fig.1). Paleozoic to Lower Triassic shallow-marine carbonates, clastic deposits, and flysch successions are unconformably overlain by Mesozoic volcano-sedimentary basin successions that developed from the Middle Jurassic onward. These basinal successions contain volcanic rocks, up to 800 m thick, as in the Dongkeng-Linjiang and Changpu-Baimianshan basins, where voluminous subalkaline basalts, rhyolites and minor high-Mg andesite-dacites were emplaced in the Middle–Late Jurassic (Wang et al., 2005). In addition, several Cretaceous to Tertiary extensional basins such as the Ji'an and Ganzhou, and Huichang, which contain red mudstone and sandstone alternating with minor basalts and andesites, are present in southern Jiangxi (BGMR, 1984; Xiong et al., 2003). This region is also characterized by widespread late Mesozoic granitoid rocks, which include peraluminous (ASI > 1.1) muscovite granite and biotite granite (Zhou and Li, 2000) as well as A-type granitic rocks such as the Jurassic Zhaibei and Potou granites, and the Quannan syenite (Chen et al., 2002; Li et al., 2003). Minor gabbroic intrusions are also present in southern Jiangxi, as exemplified by the Middle Jurassic Chebu intrusion, which consists of gabbro and amphibole gabbro with minor pyroxene anorthosite. These rocks originated from weakly enriched primitive mantle and were emplaced during lithospheric extension, probably

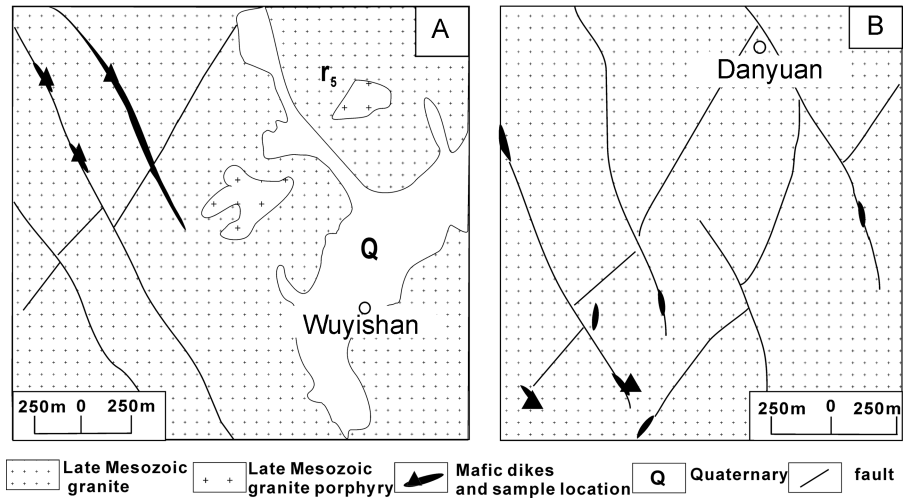

FIG. 2. Simplified geological map of Wuyishan and Danyan areas in southern Jiangxi Province, Southeast China, showing distribution of mafic dikes (modified after Chenfang 1:50,000 scale geological map).

induced by asthenospheric upwelling (Xie et al., 2005a).

Granitoid rocks are commonly cut by mafic dikes in Southeast China. A number of mafic dikes are distributed along NNE trends and intrude late Mesozoic granitoids as well as Precambrian to Cretaceous rocks in southern Jiangxi (Fig. 1). The contact between dikes and the host rocks is sharp, and most of the mafic dikes have clear chilled margins with widths ranging from several cm to tens of centimeters. NNW-, NE-, and NNE-trending mafic dikes occur in southern Jiangxi; the NNW-trending mafic dikes are dominant, with minor NE-trending mafic dikes and rare NNE-trending mafic dikes. The NNW-trending mafic dikes generally predate the NE and NNE dikes, as established for the mafic dikes in northern Guangdong (Li and McCulloch, 1998), the islands of Chinmen and Liehyu (Lan et al., 1995; Lee et al., 1998), and Gushan, East Fujian (Chen et al., 2000).

Samples were collected from the following localities in southern Jiangxi from northeast to southwest: (1) Wuyishan area south of Yunshan County; (2) Danyuan area south of Yunshan County; (3) Maopai gold ore district south of Fuzhou city; (4) Shandai area north of Yongfeng County; (5) Yanbei tin district south of Huichang County; (6) Caotaobei uranium district south of Ruijin city; and (7) Daijishan tungsten district south of Qiannan County (Fig. 1). These mafic dikes are generally distributed along fault systems and dominantly oriented along WNW trends (e.g., Danyan, Wuyishan, Maopai, Caotaobei, Yanbei, and Daijishan areas) (Fig. 2), with minor NE trends (e.g., Shandai area) (Fig. 3). The dikes vary from a few centimeters to tens of meters in width and several km to more than ten kilometers in length.

Petrography

The mafic dikes in southern Jiangxi are mainly diabase and lamprophyres. They consist mainly of plagioclase, clinopyroxene, hornblende, and biotite with minor Ti-magnetite. Their petrographic composition is similar to the dikes in northern Guangdong and Fujian provinces, as well as the islands of Chinmen and Liehyu (Lan et al., 1995; Li and McCulloch, 1998; Lee et al., 1998; Zhao et al., 2004). The mafic dikes in this study are generally fresh and were collected far away from the ore lodes in order to avoid the effects of hydrothermal alteration. However, some mafic dikes display minor alteration such as chloritization along the rims of primary phenocrysts in the diabase and carbonation in the lamprophyre.

Analytical Methods

Major-element analyses were carried out by conventional wet chemical methods at the Chemical

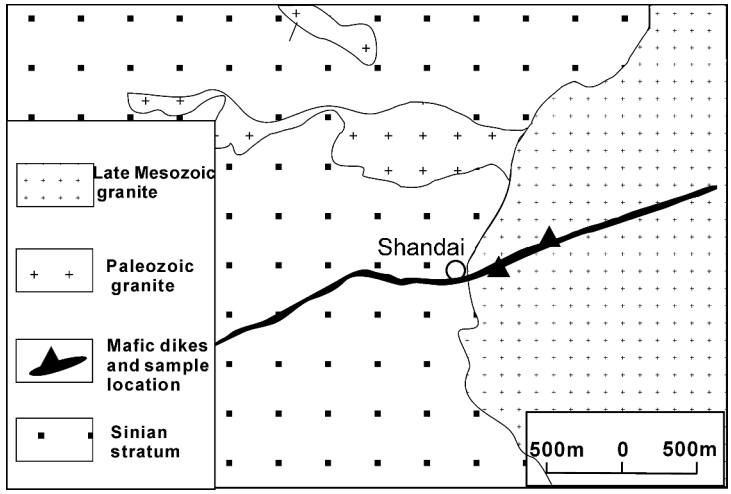

FIG. 3. Simplified geological map of Shangdai area, southern Jiangxi Province, Southeast China, showing mafic dikes and sample location (modified after Shaxiyu 1:50,000 scale geological map).

Analytical Center, Institute of Geochemistry, Chinese Academy of Sciences (IGCAS). Analytical errors for major oxides are generally less than 2%. Trace elements and rare-earth elements abundances were determined by solution ICP-MS performed at the ICP-MS Laboratory, Institute of Geochemistry, Chinese Academy of Sciences (IGCAS). The samples were digested by acid (HF + $HClO_4$) in autoclaves. Precision for most elements was typically better than 5% RSD; the measured values for Zr, Hf, Nb, and Ta were less than 10% in error compared to certified values. The detailed sample preparations, instrument operating conditions, and calibration procedures follow those established by Qi and Grégoire (2000).

For Sr-Nd isotopic analyses, sample powders (~100 mg) were dissolved in distilled HF-HNO_3 in Savillex Screwtop Teflon beakers at 150°C overnight. Sr and REE were separated on columns made of Sr and REE resins of the Eichrom Company using 0.1% HNO_3 as elutant. Separation of Nd from the REE fractions was carried out on HDEHP columns with a 0.18 N HCl elutant. The isotopic analyses were performed using a Micromass Isoprobe multicollector–ICP–MS (MC–ICPMS) at Guangzhou Institute of Geochemistry, Chinese Academy of Sciences (GIGCAS). Measured Sr and Nd isotopic ratios were normalized using an $^{86}Sr/^{88}Sr$ value of 0.1194 and a $^{146}Nd/^{144}Nd$ value of 0.7219, respectively. $^{87}Rb/^{86}Sr$ and $^{147}Sm/^{144}Nd$ ratios were calculated using the Rb, Sr, Sm, and Nd abundances measured by ICP-MS. Analyses of standards during the period of analysis are as follows: NBS987 gave $^{87}Sr/^{86}Sr = 0.710243 \pm 14$ (2σ); Shin Etou JNDi-1gave $^{143}Nd/^{144}Nd = 0.512124 \pm 11$ (2σ), equivalent to a value of 0.511860 for the La Jolla international standard (Tanaka et al., 2000). For Pb isotope analyses, sample powders were spiked and dissolved in concentrated HF at 800°C for 72 h. Lead was separated and purified by conventional anion-exchange technique (AG1 × 8, 200–400 resin) with diluted HBr. Isotopic ratios were measured using the MAT-261 mass spectrometer at the Research Center for Geological Analysis, Institute of Uranium Geology (GAIUG). In-run analytical precision for 1μg $^{208}Pb/^{206}Pb$ is better than 0.005%. Repeated analyses of NBS981 yielded $^{208}Pb/^{206}Pb = 2.1652465 \pm 0.000069$, $^{207}Pb/^{206}Pb = 0.9145100 \pm 0.000056$ and $^{204}Pb/^{206}Pb = 0.0591995 \pm 0.000013$. K-Ar dating was performed using the high-sensitivity mass spectrometer (MM1200B) at the K-Ar and ^{40}Ar-^{39}Ar Isotopic Laboratory of the Institute of Geology, China Academy of Geological Society (IGCAGS). The analytical results for Chinese standard ZBH-25 is 132.5 ± 1.6Ma (recommended age 132.7 Ma). The age calculation parameters used are $K^{40} = 0.1167\%$, $K_e = 5.811 \times 10^{-11}$/year and $K_b = 4.962 \times 10^{-10}$/year. K-Ar dating results, major chemistries, trace-element compositions, and Nd-Sr-Pb isotopic data for mafic dikes in

TABLE 1. K–Ar Dating Results for Mafic Dikes in Southern Jiangxi Province, Southeast China[1]

Sample no.	Weight, g	K, %	$^{40}Ar^*(10^{-10}mol/g)$	$^{40}Ar^*$, %	$^{40}Ar^*/^{40}K(10^{-3})$	T, Ma
DDX1	0.03002	0.91	2.3225	79.82	8.5509	141.5 ± 3.6
DDX12	0.02927	2.91	7.4762	92.48	8.6078	142.4 ± 2.5
DDX14	0.03243	1.01	8.9276	85.64	8.9276	147.5 ± 2.5
SLX5	0.02822	1.64	3.4827	85.03	7.1151	118.5 ± 2.0
CF1	0.03163	1.68	3.3164	87.11	6.6141	110.4 ± 2.1
MP4	0.03021	1.54	2.9873	82.06	6.4992	108.5 ± 1.7
SLX1	0.03008	2.37	4.4723	88.17	6.3225	105.7 ± 1.6
YFX2	0.0313	1.66	2.9671	84.82	5.9887	100.2 ± 1.6
MG4	0.03007	1.13	1.9594	87.5	5.8097	97.3 ± 1.7
CTB4	0.028	2.73	4.4744	85.65	5.4914	92.1 ± 1.5
HCX13	0.03002	3.49	5.691	90.01	5.4635	91.7 ± 1.6
HCX1	0.02858	4.07	6.1046	87.4	5.0254	84.5 ± 1.4
HCX16	0.02832	3.56	4.9592	88.04	4.6673	78.6 ± 1.2

[1]Sample numbers with prefix letters DDX, SLX, CF, YFX, and HCX are from the Daijishan, Wuyishan, Danyan, Shandai, and Yanbei areas, respectively. Samples CTB3, CTB4, CZ13, and CX5 are from the Caotaobei region. Samples WJL, MP2, MP3, MP4, MG4, and MG6 are from the Maopai area. The same sample numbers and locations are used in Tables 2, 3, and 4.

southern Jiangxi Province are listed in Tables 1–4, respectively.

Analytical Results

K-Ar dating

K-Ar dating (Table 1) yielded magmatic ages ranging from 147.5 to 78.5 Ma for the mafic dikes in southern Jiangxi, consistent with previous K-Ar dating results (Li, 1990; Li and McCulloch, 1998). For example, the K-Ar data (147.5 ± 2.5–141.5 ± 3.6 Ma) for mafic dikes in the Daijishan tungsten district in this study are consistent with previous hornblende K-Ar ages of 139.9 ±2.8 Ma in this region (Li and McCulloch, 1998). Based on the K-Ar data, the mafic dikes in southern Jiangxi were intruded during three periods: 147.5–141.5 Ma, 118.5–97.3 Ma, and 92.1–78.5 Ma. On this basis, we named these dikes Group 1, Group 2, and Group 3, respectively. *Group 1* includes mafic dikes from the Daijishan area, oriented mainly along NNW trends. *Group 2* includes mafic dikes from the Danyuan, Wuyishan, Maopai, and Shandai areas, which are widely distributed and oriented along NNW and NE trends. *Group 3* dikes are oriented along a NNW trend and include mafic dikes from the Yanbei and Caotaobei areas.

Major and trace elements

The mafic dikes span a wide range of SiO_2 (44.10–59.80%) and $K_2O + Na_2O$ (2.39–7.88%). Following the nomenclature of Le Maitre et al. (1989), the dikes may be classified as basalt, basaltic andesite, and trachybasalts, with minor basaltic trachyandesite and andesite. The total alkali versus silica classification of Irvine and Baragar (1971) shows that most samples belong to the subalkaline series, with some samples plotting in the alkaline series (Fig. 4). All mafic dikes are characterized by large variations in MgO (2.14–10.29%), CaO (0.81–11.17%) and Al_2O_3 (13.04–17.96%), and their Cr and Ni abundances range from 41.0 to 569 ppm and from 9.11 to 235 ppm, respectively, indicating the effects of fractional crystallizations during magmatic evolution (Wilson, 1989). In addition, correlations between MgO and other major oxides, as well as trace elements, suggest the important role of fractional crystallization en route to the surface (Fig. 5).

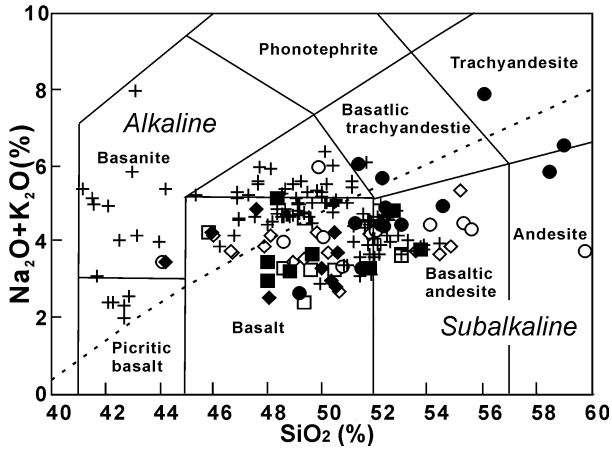

FIG. 4. Total akalis ($K_2O + Na_2O$) versus SiO_2 diagram for mafic dikes in southern Jiangxi Province, Southeast China (compositional fields from Le Maitre et al., 1989); the division between alkaline and subalkaline is after Irvine and Baragar, 1971. Symbols: open squares = 147.5–141.5 Ma mafic dikes (Group 1); open diamonds = 118.5–97.3 Ma mafic dikes (Group 2); open circles = 92.1–78.5 Ma mafic dikes (Group 3); darkened squares = ~140 Ma mafic dikes in Guangdong (Li and McCulloch, 1998); darkened diamonds = 120–100 Ma mafic dikes and basalts in Southeast China (Lapierre et al., 1997; Lee and McColluch, 1998); darkened circles = 90–80 Ma mafic dikes and basalts in Southeast China (Lan et al., 1995; Lee et al., 1998; Li and McCulloch, 1998; Xiong et al., 2003); + = Upper Cenozoic basalts in Southeast China (e.g., Flower et al., 1992; Liu et al., 1994; Qi et al., 1994; Zou et al., 2000).

For example, all samples show positive correlation between MgO and SiO_2, whereas negative correlations exists between MgO and CaO (Figs. 5A and 5B), suggesting the influence of olivine and clinopyroxene during the fractional crystallization process (Wilson, 1989). Moreover, the contents of compatible elements such as Cr and Ni decrease with MgO (Figs. 5G and 5H), also implying fractional crystallization of olivine and clinopyroxene (Wilson, 1989).

All mafic dikes in Southern Jiangxi show similar REE patterns. They are characterized by high LREE enrichment (Fig. 6), absence of negative Ce anomalies (Ce/Ce* = 0.9–1.0), and variable La_N/Yb_N (3.5–26.7) and ΣREE contents (114–433 ppm) (Table 2). Among the three Groups, Group 2 has higher LREE/HREE ratios (7.1–16.2) and ΣREE contents (168–433 ppm) than Group 1 and Group 3. LREE/HREE ratios of Group 1 and Group 3 range from 4.0 to 7.2 and from 3.9 to 13.2, respectively, with ΣREE contents of 122 to 166 ppm and from 114 to 172 ppm, for Groups 1 and 3, respectively (Fig. 6, Table 2). In addition, most of the samples have various degrees of negative Eu anomalies, such as Group 1 (ranging from 0.79 to 0.96), Group 2 (from 0.60 to 1.0), and Group 3 (0.53 to 0.82), indicating fractional crystallization of plagioclase.

In the MORB-normalized spidergrams, the mafic dikes show various degrees of enrichment in large-ion lithophile elements (LILE) (Ba, Sr, and Rb) and LREE relative to high-field-strength elements (HSFE) (Nb, Ta and Ti). Group 1 dikes have generally relatively less Nb and Ta negative anomalies than dikes in Group 2 and Group 3 (Fig. 7), and they span a wide range of Nb/La from 0.29 to 0.95. The Nb/La ratios for Group 1, Group 2 and Group 3 are 0.44–0.95, 0.34–0.58, and 0.29–0.72, respectively, which clearly distinguishes them from the Late Cenozoic basalts of Southeast China, which are related to intra-plate lithospheric extension (Fig. 7) (Peng et al., 1986; Flower et al., 1992; Liu et al., 1994; Qi et al., 1994; Chung et al., 1994, 1995; Zou et al., 2000; Ho et al., 2003). They also have relatively low Ce/Pb (0.6~16.9) and Nb/U (0.8~26.8) ratios, indicating small degrees of crustal assimilation or contamination by subducted sediments.

Sr-Nd-Pb isotopes

Age-corrected initial $^{87}Sr/^{86}Sr$ ratios and $\varepsilon_{Nd}(T)$ for these mafic dikes in southern Jiangxi span a wide range from 0.7042 to 0.7149 and from –10.8 to +5.9, respectively. As show in Figure 8, the Sr-Nd isotopic data are similar to those of late Mesozoic

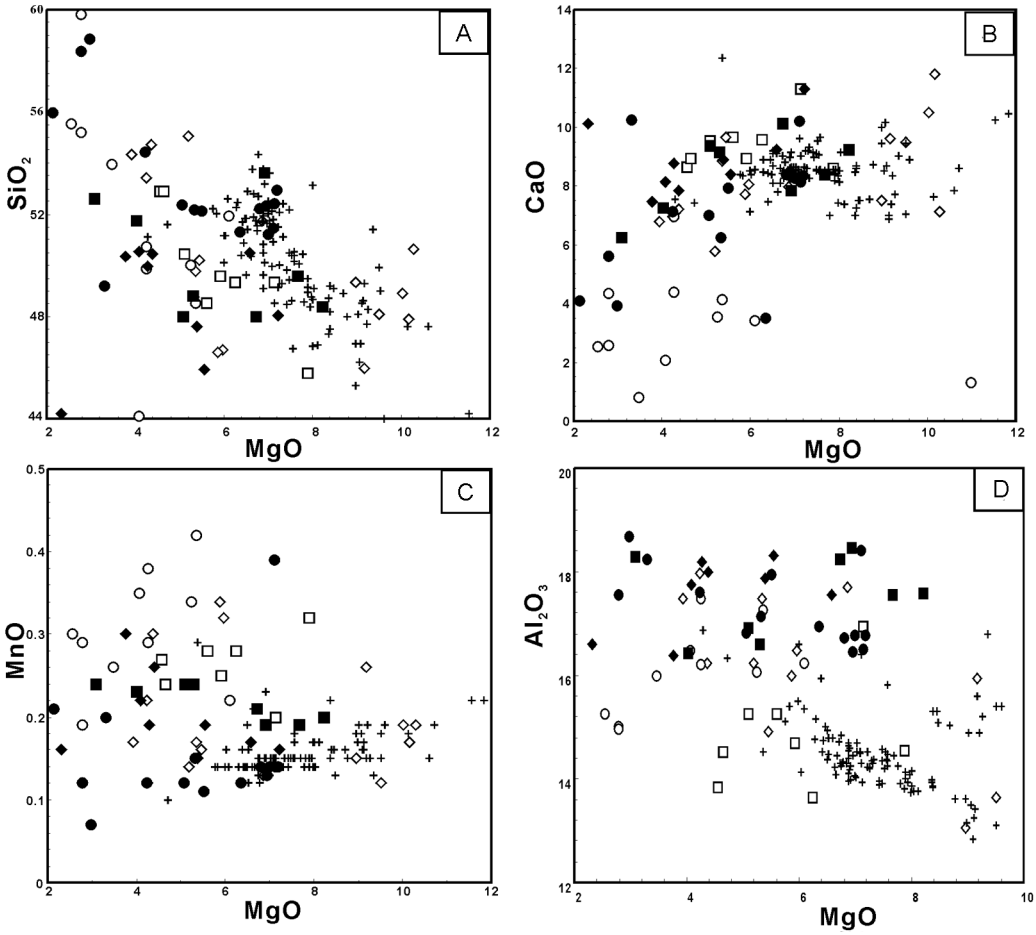

FIG. 5. Binary plots of major and trace elements versus MgO for mafic dikes, Southeast China. Symbols and references are the same as in Figure 4.

mafic dikes in Northern Gangdong, Gushan region East Fujian, and the islands of Chinmen and Liehyu (Lan et al., 1995; Li and McCulloch, 1998; Lee et al., 1998; Chen et al., 2000) as well as Cretaceous basaltic lavas in Southeast China (e.g., Lapierre et al., 1997; Xie et al., 2001; Xiong et al., 2003), but are distinct from Late Cenozoic basalts in this region (e.g. Peng et al., 1986; Tu et al., 1991; 1992; Liu et al., 1994; Chung et al., 1994, 1995; Zou et al., 2000; Ho et al., 2003; Zhu et al., 2004). The mafic dikes exhibit relatively similar Pb isotopic ratios. The $^{208}Pb/^{204}Pb$ and $^{206}Pb/^{204}Pb$ and $^{207}Pb/^{204}Pb$ ratios are 37.711–38.787, 17.819–18.400, and 15.472–15.730, for Groups 1, 2, and 3, respectively, which are similar to Cretaceous basaltic lavas in Southeast China (e.g., Xie et al., 2001; Fig. 9), and fall into the field of Late Cenozoic basalts in this region (e.g., Peng et al., 1986; Tu et al., 1991, 1992; Chung et al., 1995; Zou et al., 2000; Zhu et al., 2004).

Discussion

Petrogenesis: Crustal contamination and source enrichment?

The mafic dikes in southern Jiangxi exhibit enrichment in the LILE and LREE, and depletions in the HFSE (Fig. 7) that are consistent with crustal geochemical contamination. As discussed above, these mafic dikes are probably affected by assimilation of continental crustal material and/or contamination by subducted sediments. The geochemical characteristics of Cretaceous gabbros in the coastal

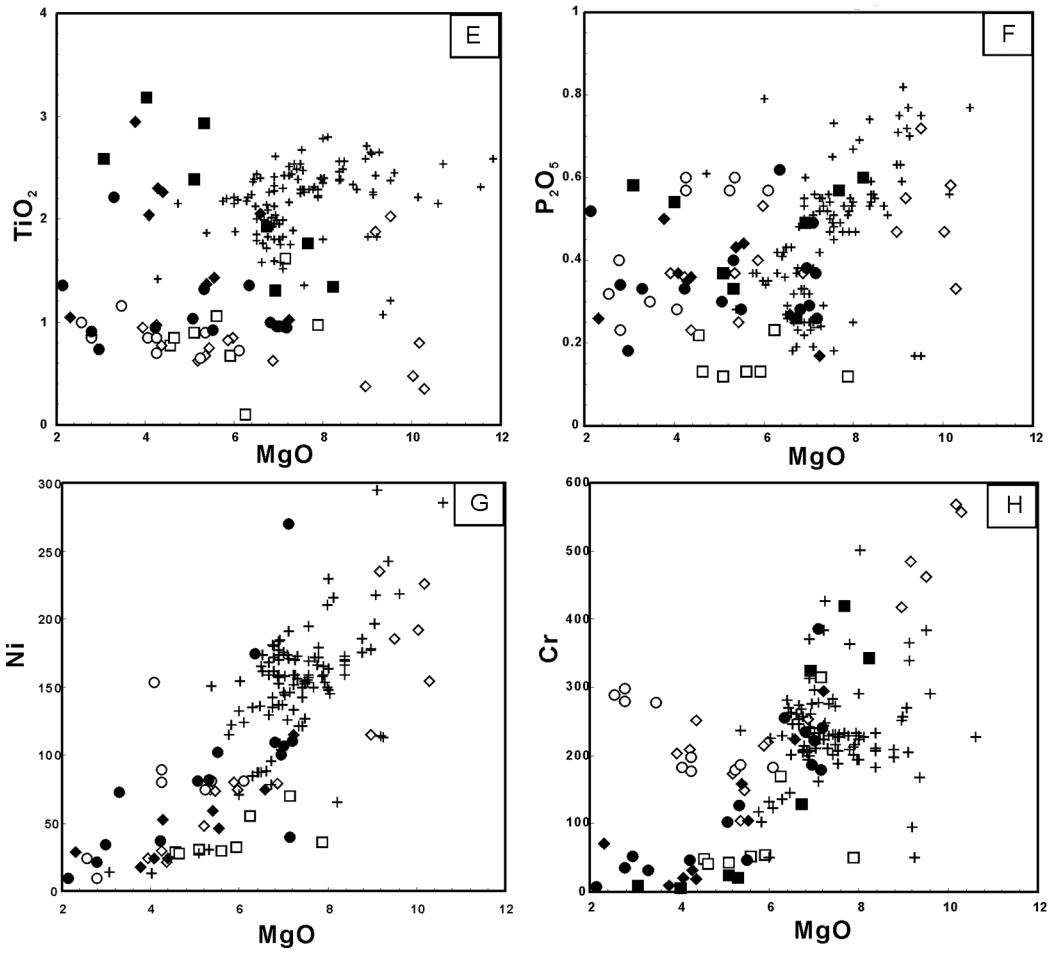

Fig. 5. *Continued.*

region of Fujian show that Precambrian crustal components played an important role in magma generation (Wang, 2002). In addition, integrated studies of field observations, geochronology, and Sr isotopic data, as well as Hf isotopes of zircon for the Tonglu and Pingtan igneous complexes in the coastal region of the provinces of Zhejiang and Fujiang, suggest that the mixing of basaltic and felsic magmas from significantly different sources beneath the crust took place in the late Mesozoic (Dong et al., 1997; Griffin et al., 2002). All these features indicate that extensive crust-mantle interaction must have occurred beneath Southeast China in the late Mesozoic.

However, several lines of evidence suggest that these mafic dikes in southern Jiangxi were not significantly affected by crustal contamination. The following need to be considered. (1) Dikes were emplaced along fault systems in an extensional tectonic regime (see below). (2) Dikes are characterized by sharp contacts with host rocks and exhibit chilled margins, suggesting that the basaltic magma probably had a short residence time in the crust and ascended quickly through the lithosphere, which did not allow significant contamination en route. (3) Dikes exhibit high concentrations of large-ion lithophile elements (LILE) such as Ba (max. of 2265 ppm), Rb (max. of 1081 ppm), and Sr (max. of 1259 ppm) (Table 2, Fig. 7), similar to Cretaceous mafic dikes in the Jiaodong Peninsula, North China craton (Yang et al., 2004), but higher than those for continental crust in East China (Ba = 678 ppm; Rb = 82

TABLE 2. Major- (%), Trace-Element (ppm), and Rare-Earth Element (ppm) Analyses for Mafic Dikes in Southern Jiangxi Province, Southeast China

Group no.:	Group 1							Group 2								
Sample no.:	DDX1	DDX4	DDX8	DDX10	DDX13	DDX14	DDX12	SLX5	SLX6	WJL	MP2	MP3	MP4	MG4	YFX-1	YFX-2
SiO_2	48.54	49.57	45.79	52.91	52.89	50.43	49.35	46.70	46.60	55.07	50.62	49.35	51.74	49.77	54.34	53.43
TiO_2	1.05	0.67	0.97	0.77	0.85	0.90	0.10	0.85	0.82	0.62	0.35	0.37	0.62	0.67	0.95	0.97
Al_2O_3	15.25	14.68	14.55	13.84	14.51	15.25	13.63	16.48	15.99	16.24	16.22	13.04	17.71	17.47	17.47	17.96
Fe_2O_3	5.48	5.66	5.85	5.99	4.87	6.19	3.10	3.88	3.81	1.74	3.00	3.21	3.05	3.5	3.87	3.95
FeO	7.49	7.70	8.80	7.10	6.95	7.00	8.98	5.10	4.95	6.60	6.15	5.90	4.90	5.7	4.2	4.7
MnO	0.28	0.25	0.32	0.27	0.24	0.24	0.28	0.32	0.34	0.14	0.19	0.15	0.13	0.17	0.17	0.22
MgO	5.60	5.92	7.88	4.56	4.65	5.10	6.25	5.97	5.87	5.19	10.29	8.96	6.87	5.35	3.93	4.24
CaO	9.64	8.93	8.60	8.63	8.93	9.51	9.59	8.05	7.71	5.77	7.13	7.50	7.95	8.87	6.8	6.96
Na_2O	2.21	2.39	1.52	1.95	2.37	2.36	1.90	2.15	2.02	2.86	1.77	2.29	2.69	2.92	2.27	2.29
K_2O	1.11	0.87	2.72	1.72	1.28	0.91	2.72	1.58	1.72	2.48	0.93	1.27	1.51	1.31	1.4	1.47
P_2O_5	0.13	0.13	0.12	0.22	0.13	0.12	0.23	0.53	0.40	0.37	0.33	0.47	0.37	0.37	0.37	0.36
LOI	2.15	2.20	2.30	1.75	1.72	1.40	2.70	3.87	3.61	2.90	2.73	4.04	1.86	3.36	3.64	2.86
CO_2	0.65	0.50	–	–	–	–	0.95	4.25	5.82	–	–	3.00	–	–	–	–
Sum	99.58	99.47	99.42	99.71	99.39	99.41	99.78	99.73	99.66	99.98	99.71	99.55	99.40	99.46	99.41	99.41
Sc	33.4	31.3	44.4	37.3	35.2	34.0	34.5	25.3	26.6	19.6	30.6	30.0	21.0	22.5	25.8	26.8
Cr	53.0	53.7	49.7	47.6	41.0	42.5	169	219	214	173	558	418	254	105	203	209
V	463	452	386	376	383	440	377	372	402	231	194	275	236	246	82.4	98.8
Co	88.0	104	88.3	103	132	94.2	50.5	51.5	54.8	61.6	77.9	83.9	78.8	62.2	70.8	77.6
Ni	29.5	32.3	35.9	28.5	27.5	29.9	55.5	74.6	80.2	47.7	154	115	78.8	74.5	23.8	29.6
Pb	8.10	8.10	5.80	8.95	8.26	7.5	12.0	8.13	7.00	6.92	16.23	8.38	9.42	5.52	11.6	10.1
U	0.782	0.784	0.947	1.05	0.807	0.717	0.761	1.13	1.21	1.24	0.731	0.763	0.975	0.821	1.2	1.13
Sr	364	401	264	344	348	381	270	680	731	524	449	630	812	911	339	330
Rb	392	229	783	598	302	225	1081	95.4	107	37.9	24.6	47.6	54.2	35.9	37.5	68.9

Ba	119	97.0	187	184	149	89.1	243	630	479	793	419	746	729	617	444	464
Th	2.69	2.77	3.22	3.26	2.50	2.53	3.11	5.11	5.48	5.92	4.13	3.90	4.74	3.93	8.73	8.44
Ta	0.977	1.20	1.45	1.24	1.28	1.10	1.76	0.554	0.594	0.930	0.640	0.670	0.800	1	0.777	0.766
Nb	15.2	16.8	19.4	18.4	16.7	15.9	16.4	12.7	14.5	19.3	14.2	14.8	17.1	20.2	15.2	15.5
Zr	160	174	200	198	158	160	151	144	156	155	116	112	131	143	174	177
Hf	5.09	5.48	6.24	6.89	6.21	4.91	4.9	4.01	4.05	4.71	3.71	4.03	4.27	4.13	5.32	5.6
Y	36.5	40.2	48.4	46.2	38.4	38.4	29.7	21.8	24.0	26.3	21.9	28.9	27.8	27.1	31.3	31.1
La	17.4	19.2	22.7	25.5	17.5	17.8	37.2	44.85	48.6	36.1	30.3	31.2	36.3	35.3	33.2	33.7
Ce	42.1	46.4	54.7	58.6	41.3	42.7	62.9	84.7	90.2	73.4	62.7	63.4	75.7	74.1	66.4	71.2
Pr	5.49	5.98	7.06	7.31	5.39	5.33	7.07	9.11	9.70	8.48	7.11	7.91	8.63	8.69	7.95	7.75
Nd	25.9	27.2	32.1	33.5	24.7	25.6	27.1	34.5	36.0	35.4	30.4	33.9	36.8	36.7	31.8	31.4
Sm	6.39	7.38	8.54	7.87	6.24	6.94	6.22	5.65	5.84	7.02	5.55	7.12	6.69	6.84	6.56	6.26
Eu	2.06	2.19	2.48	2.49	2.01	1.94	1.59	1.56	1.74	1.89	1.57	1.97	2.06	2.1	1.22	1.29
Gd	6.67	7.00	8.86	8.24	6.86	6.74	5.88	5.28	5.61	5.81	4.79	6.47	6.51	6.54	5.77	6.12
Tb	1.13	1.29	1.56	1.39	1.19	1.12	0.916	0.755	0.798	0.893	0.720	0.979	0.970	0.943	0.939	0.853
Dy	7.3	7.57	9.45	9.09	7.34	7.71	5.45	4.22	4.17	5.07	4.08	5.64	5.27	5.14	5.77	5.61
Ho	1.39	1.52	1.78	1.74	1.33	1.42	1.09	0.75	0.82	0.929	0.788	1.05	0.903	0.949	1.08	1.07
Er	3.79	4.22	4.91	4.65	3.86	3.77	2.90	2.02	2.17	2.59	2.14	2.79	2.68	2.44	3.13	3.03
Tm	0.511	0.528	0.652	0.592	0.546	0.534	0.373	0.25	0.29	0.339	0.287	0.387	0.323	0.334	0.438	0.411
Yb	3.38	3.67	4.35	4.23	3.44	3.48	2.69	1.96	1.96	2.45	2.08	2.59	2.33	2.45	3.02	3.01
Lu	0.457	0.536	0.583	0.592	0.486	0.509	0.371	0.288	0.311	0.331	0.308	0.351	0.309	0.344	0.468	0.431
ΣREE	124	135	160	166	122	126	162	196	208	181	153	166	185	183	168	172
δEu	0.96	0.92	0.87	0.94	0.94	0.86	0.79	0.86	0.92	0.88	0.91	0.87	0.94	0.96	0.6	0.63
δCe	1	1	1.0	1.0	1.0	1.0	0.9	1.0	1.0	1.0	1.0	0.9	1.0	1.0	1.0	1.0

Table continues

TABLE 2. *Continued*

Group no.:	Group 2						Group 3									
Sample no.:	MG6	SLX1	CF4	CF1	CF3	CF6	HCX1	HCX5	HCX9	HCX10	HCX13	HCX16	CTB3	CTB4	CZ13	CX5
SiO_2	50.22	54.73	47.87	48.90	45.97	48.07	49.84	50.00	48.54	51.95	44.10	50.73	55.18	55.51	59.80	53.94
TiO_2	0.74	0.77	0.80	0.47	1.88	2.03	0.70	0.65	0.90	0.72	0.85	0.85	0.87	1.00	0.85	1.15
Al_2O_3	14.92	16.24	11.81	13.64	15.95	13.64	17.47	16.07	17.26	16.24	16.48	16.22	15.01	15.25	14.97	15.99
Fe_2O_3	4.60	3.50	3.16	3.04	1.56	1.04	3.33	3.48	3.55	3.25	3.28	3.79	3.95	3.66	4.84	3.18
FeO	5.98	4.00	5.52	5.50	6.10	6.25	4.10	4.20	4.05	4.10	7.00	4.50	6.69	6.50	5.20	7.54
MnO	0.16	0.30	0.17	0.19	0.26	0.12	0.38	0.34	0.42	0.22	0.35	0.29	0.29	0.30	0.19	0.26
MgO	5.45	4.37	10.17	10.03	9.17	9.51	4.26	5.24	5.36	6.10	4.07	4.26	2.79	2.55	2.78	3.47
CaO	9.64	7.21	11.79	10.50	9.62	9.48	3.53	4.12	3.40	2.08	4.40	4.35	2.54	2.59	0.81	1.29
Na_2O	2.57	1.71	1.44	1.78	2.21	2.61	2.27	1.47	1.41	1.63	0.19	0.23	2.79	2.16	1.94	2.34
K_2O	1.15	2.15	2.42	1.69	1.94	1.56	3.67	2.64	2.57	2.65	3.29	3.13	1.72	2.16	1.83	2.1
P_2O_5	0.25	0.23	0.58	0.47	0.55	0.72	0.60	0.57	0.60	0.57	0.28	0.57	0.23	0.32	0.40	0.3
LOI	3.62	2.61	3.68	3.56	2.40	3.80	4.63	5.90	6.89	5.80	9.07	4.70	3.93	3.93	2.84	5.48
CO_2	–	2.05	–	–	1.70	0.99	5.04	5.10	4.83	4.10	6.30	6.34	3.61	3.75	3.12	2.5
Sum	99.30	99.88	99.41	99.77	99.31	99.82	99.42	99.78	99.78	99.41	99.66	99.96	99.60	99.68	99.57	99.54
Sc	22.7	32.3	31.3	32.6	31.6	33.1	16.2	16.2	16.8	17.9	20.9	18.0	31.0	29.8	29.1	21.1
Cr	149	252	569	609	484	462	178	179	187	182	182	198	279	288	298	277
V	251	205	244	264	239	256	181	180	188	208	271	178	44.0	76.0	48.0	33.7
Co	60.3	71.6	64.8	66.8	58.3	52.4	60.2	46.7	38.3	51.8	49.6	42.9	59.3	53.3	48.8	45.2
Ni	73	20.7	226	192	235	185	79.6	74.7	80.5	80.5	153.6	89.1	9.11	23.5	7.53	5.37
Pb	17.3	19.7	11.4	12.8	11.2	11.8	12.0	113	12.6	10.6	24.3	5.97	28.9	93.9	28.2	36.7
U	0.556	1.56	2.42	1.26	2.61	1.42	1.44	1.6	1.5	1.9	1.8	1.81	20.1	17.2	17.4	6.89
Sr	635	424	1259	1016	1190	1000	439	233	217	197	110	119	165	130	36.8	71.8
Rb	35.1	168	140	67.3	154	62.2	261	239	150	262	430	292	117	167	74.6	46.7

Ba	525	653	2265	1684	2014	1575	858	533	464	533	263	321	430	479	312	326
Th	2.78	8.73	14.9	7.72	16.2	8.29	5.64	6.23	6.14	5.94	6.69	6.32	12.2	12.1	8.92	9.65
Ta	0.840	0.630	1.84	1.36	1.94	1.45	0.470	0.478	0.473	0.486	0.390	0.493	0.966	0.961	1.03	0.951
Nb	14.9	11.8	41.5	29.3	42.8	29.5	9.20	9.70	9.93	9.98	7.14	11.0	14.2	14.1	15.6	14.8
Zr	117	139	207	163	214	164	138	146	148	145	114	159	176.44	178.85	195.60	183.2
Hf	3.68	4.57	5.29	4.54	5.51	4.19	4.49	4.44	4.54	4.60	3.75	4.43	5.49	5.60	5.87	5.54
Y	26.2	29.0	34.1	32.5	33.0	24.9	15.8	17.0	17.8	16.2	24.6	33.1	39.0	35.5	30.8	32.3
La	25.5	38.6	96.5	60.0	102	54.5	26.7	33.9	29.0	29.8	24.0	31.7	30.2	29.8	26.7	20.6
Ce	54.5	74.7	185	123	189	116	59.4	65.5	58.1	62.5	51.8	65.7	60.6	60.0	52.3	40.1
Pr	6.64	7.88	20.4	14.5	20.5	13.0	6.70	8.64	7.19	7.50	6.21	8.80	7.25	7.09	6.50	5.11
Nd	27.8	29.1	80.2	58.2	80.5	51.9	27.5	34.3	28.9	30.2	25.9	36.8	29.5	28.8	26.9	21.7
Sm	5.88	5.24	13	10.2	13.2	9.17	5.08	6.41	5.49	5.01	4.97	7.51	6.63	6.23	5.70	5.12
Eu	2.00	1.35	2.97	2.37	2.87	2.15	1.32	1.70	1.39	1.42	1.32	1.71	1.40	1.37	0.970	0.846
Gd	5.94	5.3	10	8.43	9.77	7.39	4.62	5.09	4.85	4.53	4.76	6.55	6.31	6.02	5.41	4.99
Tb	0.886	0.810	1.30	1.14	1.31	0.986	0.525	0.688	0.673	0.659	0.746	0.989	1.15	1.08	0.954	0.858
Dy	5.05	5.03	6.58	6.42	6.76	5.00	3.07	3.43	3.33	3.26	4.23	5.69	7.47	6.07	5.94	5.95
Ho	0.942	1.012	1.23	1.18	1.12	0.91	0.571	0.614	0.616	0.581	0.766	1.01	1.45	1.27	1.15	1.12
Er	2.39	2.75	3.11	2.92	3.02	2.32	1.45	1.55	1.68	1.53	2.17	2.93	3.79	3.72	3.41	3.45
Tm	0.306	0.369	0.378	0.365	0.382	0.317	0.199	0.207	0.227	0.202	0.307	0.382	0.551	0.49	0.557	0.481
Yb	2.18	2.6	2.63	2.35	2.49	2.04	1.36	1.55	1.52	1.35	1.84	2.66	4.12	3.80	3.94	3.58
Lu	0.326	0.401	0.361	0.355	0.347	0.295	0.185	0.265	0.216	0.211	0.269	0.400	0.582	0.534	0.518	0.531
ΣREE	140	175	424	291	433	266	139	164	143	149	129	173	161	156	141	114
δEu	0.95	1.03	0.78	0.77	0.76	0.74	0.77	0.82	0.88	0.8	0.89	0.82	0.73	0.65	0.67	0.53
δCe	1.0	1.0	1.0	1.0	1.0	0.9	1.0	1.0	0.9	0.9	1.0	1.0	0.9	1.0	1.0	0.9

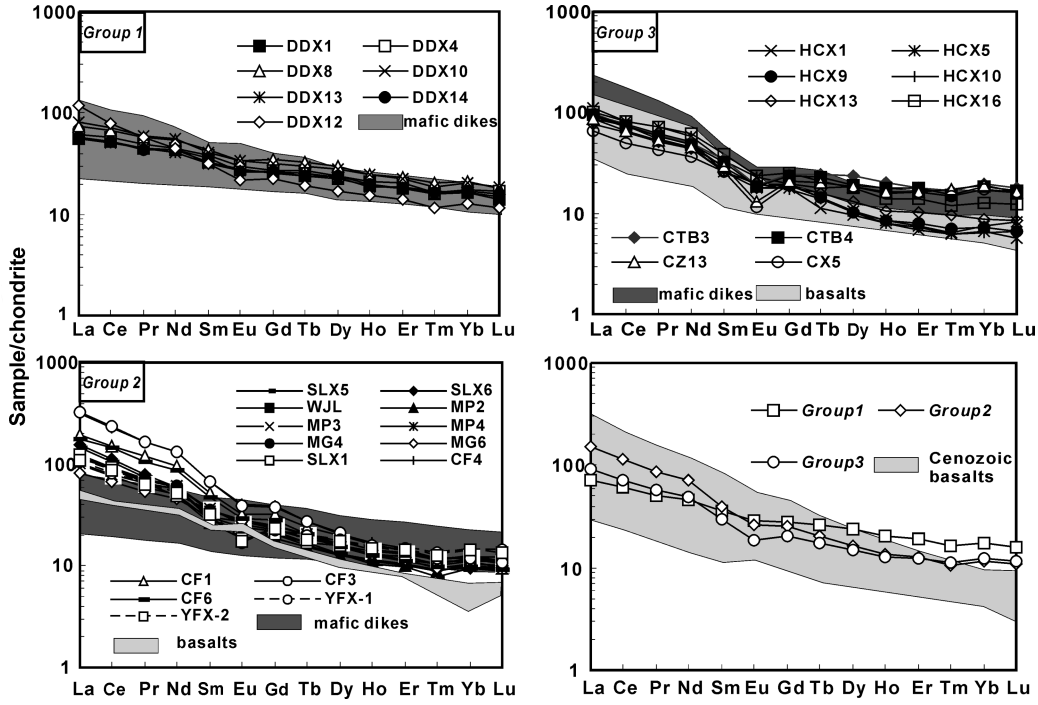

FIG. 6. Chondrite-normalized REE pattterns for mafic dikes. Normalization values are after Rollinson (1993). Symbols and references are the same as in Figure 4.

ppm; Sr = 266 ppm; Gao et al., 1998). These data indicate that crustal assimilation may not have played a significant role in their petrogenesis. (4) Analyzed samples display high and variable initial $^{87}Sr/^{86}Sr$ ratios and $\varepsilon_{Nd}(T)$ values, similar to those of Cretaceous basalts in the coastal region (e.g. Xie et al., 2001) and mafic dikes from Northern Guandong and the islands of Chinmen and Liehyu (Lan et al., 1995; Li and McCulloch, 1998; Lee et al., 1998) as well as Gushan, Eastern Fujian (Chen et al., 2000) in Southeast China (Fig. 8). Geochemical and Sr-Nd-Pb-O isotopic systematics and numerical modeling demonstrate that the magmas responsible for the Cretaceous basalts in the coastal area and mafic dikes in northern Guandong and the islands of Chinmen and Liehyu were not substantially modified by crustal contamination. Therefore, these Sr-Nd isotopic characteristics, shown in Figure 8, indicate that the mafic dikes in southern Jiangxi were probably not affected by a large proportion of crustal contamination en route to the surface. (5) Pb is significantly enriched in continental crust relative to mantle-derived melts, such as MORB and OIB. Consequently, mantle-derived basalts contaminated by crustal material will have enhanced Pb isotopic compositions. The $^{206}Pb/^{204}Pb$, $^{207}Pb/^{204}Pb$, and $^{208}Pb/^{204}Pb$ ratios of these mafic dikes in this study show narrow variations for the three groups of 18.171, 15.579, and 38.365 on average. These values are similar to least-contaminated Upper Cenozoic basalts in Southeast China (Zou et al., 2000; Fig. 9). (6) The SiO_2 and MgO contents of continental crust are generally higher than those of mantle-derived melts, and rocks that are significantly influenced by crustal contamination would exhibit positive correlation among Sr-Nd isotopic compositions and SiO_2 or MgO (Piccrillo et al., 1989). However, such correlations between $^{87}Sr/^{86}Sr$ or $^{144}Nd/^{143}Nd$ and crust-derived elements such as SiO_2 or MgO (Fig. 10), are not found in the mafic dikes from Southern Jiangxi. In addition, positive correlations of $^{87}Sr/^{86}Sr$ or $^{144}Nd/^{143}Nd$ with 1/Sr or 1/Nd are not recorded in these mafic dikes (Table 3).From the above, we conclude that the geochemical and isotopic characteristics of the Southern Jiangxi mafic dikes are indicative of contamination by subducted

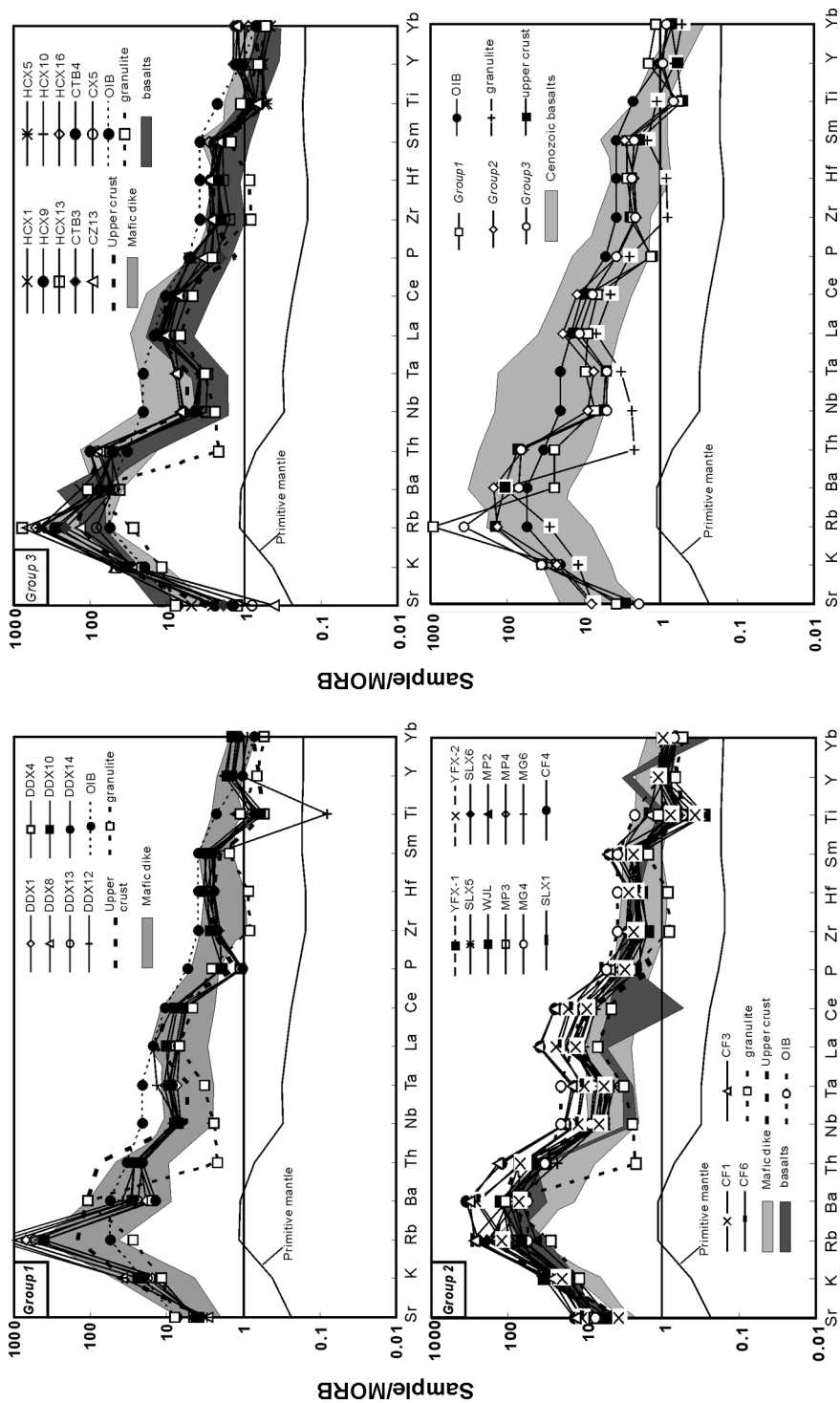

FIG. 7. MORB-normalized incompatible element spider diagrams for mafic dikes. MORB, primitive mantle, and OIB values are after Sun and McDonough (1989); upper crust and lower crust granulite in the Cathaysian block are after Gao et al. (1998) and Yu et al. (2003), respectively. Symbols and references are the same as in Figure 4.

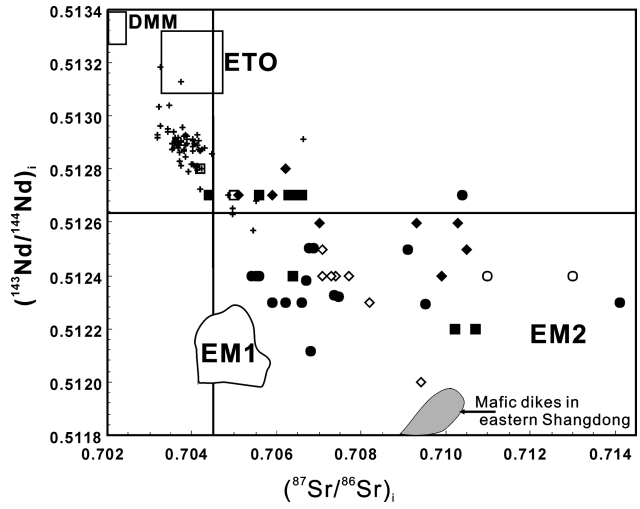

FIG. 8. Nd and Sr isotopic variation diagram for mafic dikes. DDM, EM1, and EM 2 are from Zindler and Hart (1986). Abbreviations: ETO = East Twain ophiolite. N-type basalts field is from Jahn (1986). Fields of Cretaceous mafic dikes in eastern Shandong Province are from Yang et al. (2004). Symbols: open squares = 147.5–141.5 Ma mafic dikes (Group 1); open diamonds = 118.5–97.3 Ma mafic dikes (Group 2); open circles = 92.1–78.5 Ma mafic dikes (Group 3); darkened squares = ~140 Ma mafic dikes in Guangdong (Li and McCulloch, 1998); darkened diamonds = 120–100 Ma mafic dikes and basalts in Southeast China (Li, 1990; Lapierre et al., 1997; Li and McCulloch, 1998); darkened circles = 90–80 Ma mafic dikes and basalts in Southeast China (Lan et al., 1995; Lee et al., 1998; Li and McCulloch, 1998; Chen et al., 2000; Xiong et al., 2003); + = Upper Cenozoic basalts in Southeast China (e.g., Flower et al., 1992; Liu et al., 1994; Qi et al., 1994; Zou et al., 2000).

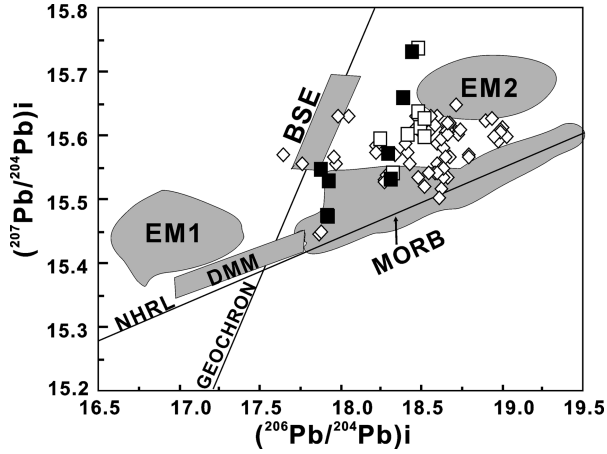

FIG. 9. Initial $^{206}Pb/^{204}Pb$ and $^{207}Pb/^{204}Pb$ variation diagram for mafic dikes. DMM, MORB, EM1, and EM2 after Zindler and Hart (1986). Symbols: darkened squares = mafic dikes in southern Jiangxi Province (this study); open diamonds = Upper Cenozoic basalts in Southeast China (Peng et al., 1986; Tu et al., 1991, 1992; Chung et al., 1995; Zou et al., 2000); open squares = Cretaceous basalts in Southeast China (Xie et al., 2001).

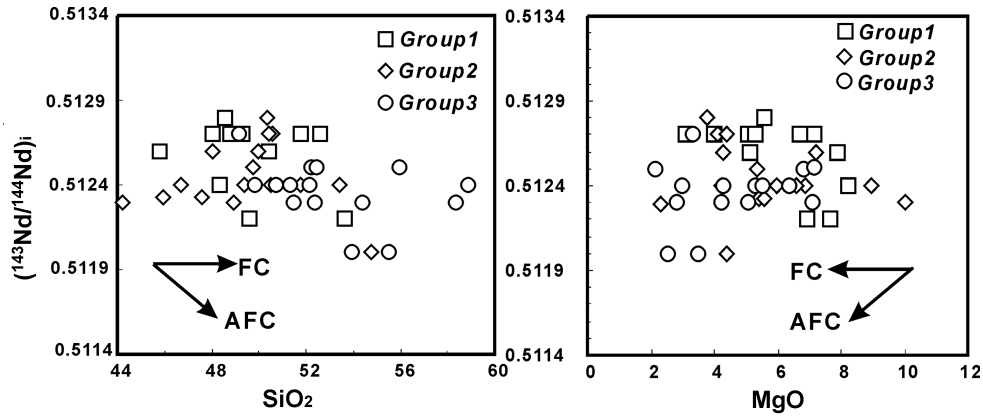

FIG. 10. Initial $^{144}Nd/^{143}Nd$ and SiO_2 and MgO variation diagram for mafic dikes. Symbols are the same as those in Figure 4.

sediments and inherited from mantle sources beneath the crust.

Magma source

As discussed above, the mafic dikes in southern Jiangxi exhibit a wide range of geochemical and isotopic compositions (Tables 2–3; Figs. 4–9). These compositions imply that the basaltic magma responsible for these dikes was derived from either the partial melting of a homogeneous or heterogeneous mantle source. As shown in Table 2, the Th/Ta and Ce/Nb ratios of the mafic dikes range from 0.08 to 0.41 and 2.72 to 7.25, suggesting that they were probably derived from a heterogeneous mantle source. If this had not been the case, then most of incompatible trace elements ratios for these dikes should be similar, because of the similar geochemical behavior in these trace elements during magmatic evolution (cf. Rollinson, 1993). In addition, the southern Jiangxi dikes were enriched in LILE and LREE, as well as Sr-Nd-Pb isotopes (Tables 2–3; Figs. 6–9), clearly distinguishing them from MORB and OIB (Sun and McDonough, 1989). Therefore, the Southern Jiangxi dikes were probably derived from heterogeneous enriched mantle and underwent LILE and LREE enrichment before or during basaltic magma generation. Two kinds of metasomatic events may be responsible for such geochemical and isotopic signatures: (1) a subduction-related metasomatic event with LILE and LREE and isotope-enriched fluid/melt derived from subducted sediment (e.g., McCulloch and Gamble, 1991); and (2) a metasomatic event by minor carbonate-rich melt/fluid, especially in the lamprophyres, that may have originated from the asthenospheric mantle (e.g., Rock et al., 1990). Both Zr and Hf show similar geochemical behavior due to their nearly identical ionic radii and charges (Jochum et al., 1989); therefore, Zr/Hf values remain constant during petrogenetic processes except for fluid metasomatism (e.g., Dupuy et al., 1992; Rudnick et al., 1993). The mafic dikes of southern Jiangxi exhibit low Zr/Hf ratios, ranging from 25.4 to 39.1 lower than chondritic values, which suggests that the mantle source for these dikes had not been infiltrated by carbonate-rich fluid/melt from the asthenospheric mantle (Dupuy et al., 1992). Consequently, the late Mesozoic mafic dikes in southern Jiangxi originated from an enriched lithospheric mantle induced by subduction-related fluids, which must have occurred shortly before the emplacement of mafic dikes (Li and McCulloch, 1998; Xu et al., 2003). With regard to amphibole, phlogopite has much higher partition coefficients for Rb and Ba but lower for Sr than amphibole, so melts in equilibrium with phlogophite are expected to have higher Rb/Sr and lower Ba/Rb ratios than those from those from amphibole-bearing sources (Furman and Graham, 1999). In Table 2, most mafic dikes in southern Jiangxi display high Rb/Sr(>0.1) and low Ba/Rb (<20), indicating their mantle source consisted mainly of phlogopite peridotites (Furman and Graham, 1999).

Several mantle components have been identified from isotopic studies of mid-ocean ridge basalts (MORB) and ocean island basalts (OIB), such as

TABLE 3. Sr and Nd Isotopic Compositions of Late Mesozoic Mafic Dikes in Southern Jiangxi Province, Southeast China[1]

Sample no.	Sm	Nd	$^{147}Sm/^{144}Nd$	$^{143}Nd/^{144}Nd$	2δ	$(^{143}Nd/^{144}Nd)_i$	$\varepsilon_{Nd}(T)$	Rb	Sr	$^{87}Rb/^{86}Sr$	$^{87}Sr/^{86}Sr$	2δ	$(^{87}Sr/^{86}Sr)_i$	$\varepsilon_{Sr}(T)$
DDX1	6.39	25.9	0.1640	0.512910	0.000010	0.5128	5.9	392	364	3.117	0.704608	0.000010	0.7042	–2.8
DDX8	8.54	32.1	0.1608	0.512760	0.000009	0.5126	3.0	–	–	–	–	–	–	–
DDX14	6.94	25.6	0.1639	0.512763	0.000010	0.5126	3 .0	–	–	–	–	–	–	–
BD-4	3.46	12.01	0.1739	0.512887	0.000005	0.5127	5.3	22.7	188	0.3491	0.705549	0.000011	0.7050	9.0
SLX5	5.65	34.5	0.0990	0.512472	0.000008	0.5124	–1.7	95.4	680	0.4059	0.708075	0.000014	0.7074	43
CF1	10.2	58.2	0.1060	0.512329	0.000008	0.5123	–4.8	67.3	1016	0.1917	0.708497	0.000014	0.7082	54
YFX2	6.26	31.4	0.1205	0.512459	0.000009	0.5124	–2.5	68.9	330	0.6401	0.707985	0.00001	0.7071	38
MP3	7.12	33.9	0.1270	0.512480	0.000007	0.5124	–2.1	47.6	630	0.2186	0.707976	0.000011	0.7077	46
MP4	6.69	36.8	0.1099	0.512462	0.000008	0.5124	–2.2	54.2	812	0.1931	0.707562	0.000013	0.7073	41
MG4	6.84	36.7	0.1127	0.512569	0.000008	0.5125	–0.3	35.9	911	0.1140	0.707309	0.000013	0.7071	39
SLX1	26.9	48.5	0.3350	0.512221	0.000008	0.5120	–10.0	168	424	1.149	0.71109	0.000017	0.7094	71
HCX1	5.08	27.5	0.1170	0.512459	0.000009	0.5124	–2.6	261	439	1.720	0.713085	0.000011	0.7110	94
HCX16	7.51	36.8	0.1234	0.512467	0.000007	0.5124	–2.5	292	119	7.110	0.721584	0.000012	0.7130	122
CTB4	6.23	28.8	0.1308	0.512047	0.000008	0.5120	–10.8	–	–	–	–	–	–	–
CX5	5.12	21.7	0.1427	0.512056	0.000009	0.5120	–10.8	–	–	–	–	–	–	–

[1] "–" = not analyzed. Sample BD-4 is from Li and McCulloch, 1998. $^{143}Nd/^{144}Nd$ and $^{87}Sr/^{86}Sr$ are calculated using K-Ar ages. $(^{87}Sr/^{86}Sr)^0_{UR} = 0.7045$; $(^{87}Rb/^{86}Rb)^0_{UR} = 0.0827$; $(^{143}Sm/^{144}Nd)^0_{CHUR} = 0.51238$; $(^{143}Nd/^{144}Nd)^0_{CHUR} = 0.1967$; $M_{Rb} = 1.42 \times 10^{-11}$/year; $M_{Sm} = 6.54 \times 10^{-12}$/year; see Rollinson, 1993.

DMM (depleted MORB mantle, high $^{143}Nd/^{144}Nd$, low $^{87}Sr/^{86}Sr$ and $^{206}Pb/^{204}Pb$), HIMU (high U/Pb ratio), EM1 (enriched mantle with intermediate $^{87}Sr/^{86}Sr$, low $^{143}Nd/^{144}Nd$, and $^{206}Pb/^{204}Pb$), and EM2 (enriched mantle characterized by high $^{206}Pb/^{204}Pb$, high $^{87}Sr/^{86}Sr$ and intermediate $^{143}Nd/^{144}Nd$) (Zindler and Hart, 1986). As shown in Figure 9, the southern Jiangxi dikes share transitional Pb isotopic compositions between DMM or MORB and EM 2, suggesting mixing between DMM and EM 2 components. Their isotopic characteristics can generally be explained as dominantly the EM 2 mantle with minor the depleted asthenospheric mantle, best illustrated by the $^{87}Sr/^{86}Sr$ vs. $^{206}Pb/^{204}$ Pb (Fig. 11) and $^{143}Nd/^{144}Nd$ vs.$^{206}Pb/^{204}$ Pb diagrams (Fig. 12). It has been proposed the EM 2 component in Southeast China may have been derived from continental lithospheric mantle such as Tungchihsu Group 2 rocks (Ho et al., 2000), and the EM 2 continental lithospheric mantle was related to the subduction of the Pacific plate beneath the Eurasian plate in the Mesozoic (Chung et al., 1995) or might have been affected by sediments associated with a Paleo-subduction zone (Ho et al., 2003). In addition, continental lithospheric mantle reservoirs in the extensional provinces may have diverse origins and distinct compositions in Eastern China (Chung et al., 1995); large variations in elemental and Sr-Nd isotopic compositions for these mafic dikes in this study are probably related to highly heterogeneous lithospheric mantle beneath the crust in Southeast China during late Mesozoic time (Lan et al., 1995; Lee et al., 1998; Chen et al., 2000; Xie et al., 2001; Zhao et al., 2004).

We believe that the South China Lithospheric Mantle in Southeast China during the late Mesozoic was dominated by an enriched lithospheric mantle (EM 2) component, mixed with minor proportions of depleted mantle (Li and McCulloch, 1998). This is supported by recent studies of peridotitic xenoliths, which suggest that lithospheric mantle beneath the Cathaysian block is dominated by Phanerozoic garnet and spinel lherzolites, and that a minor proportion of Proterozoic mantle may have been preserved in the upper levels (Zheng et al., 2004).

TABLE 4. Pb Isotopic Compositions of Late Mesozoic Mafic Dikes in Southern Jiangxi Province, Southeast China[1]

				Measured Pb isotopic ratio						Calculated initial Pb isotopic ratios		
Sample	U	Pb	Th	$^{208}Pb/^{204}Pb$	2σ	$^{207}Pb/^{204}Pb$	2σ	$^{206}Pb/^{204}Pb$	2σ	$^{206}Pb/^{204}Pb$	$^{208}Pb/^{204}Pb$	$^{207}Pb/^{204}Pb$
SLX5	1.13	8.13	5.11	38.698	26	15.576	10	18.38	12	18.214	38.455	15.57
MP4	0.975	9.42	4.74	38.11	13	15.477	5	17.991	5	17.88	37.935	15.472
SLX1	1.56	19.7	8.72	38.45	150	15.531	61	17.969	70	17.886	38.299	15.527
CF1	1.26	12.8	7.72	38.186	32	15.55	13	17.927	15	17.819	37.973	15.545
YFX2	1.13	10.1	8.44	39.066	8	15.663	3	18.469	4	18.356	38.792	15.658
HCX1	1.44	12.0	5.64	37.839	15	15.536	6	18.377	7	18.277	37.711	15.532
HCX16	1.81	5.97	6.32	39.06	32	15.742	13	18.641	15	18.4	38.787	15.730

[1]Initial Pb ratios are calculated using K-Ar ages; $M_{U238} = 1.55125 \times 10^{-10}$/year; $M_{U235} = 9.8485 \times 10^{-10}$/year, $M_{Th232} = 4.9475 \times 10^{-11}$/year; see Rollinson, 1993.

Tectonic Implications

Lithospheric extension

Igneous rock suites are closely associated with specific tectonic settings. The tectonic setting of late Mesozoic igneous provinces in Southeast China

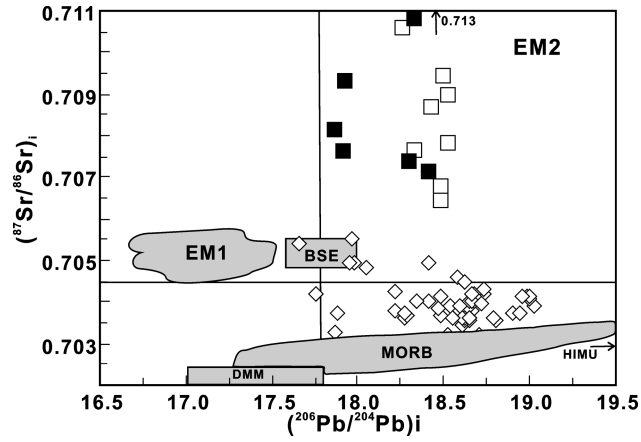

FIG. 11. Initial $^{206}Pb/^{204}Pb$ and $^{87}Sr/^{86}Sr$ variation diagram for mafic dikes. Symbols are the same as those in Figure 4.

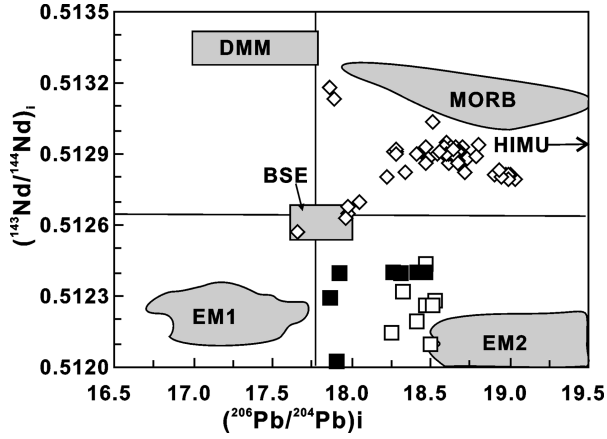

FIG. 12. Initial $^{206}Pb/^{204}Pb$ and $^{144}Nd/^{143}Nd$ variation diagram for mafic dikes. Symbols are the same as those in Figure 4.

remains controversial (Li, 2000; Zhou and Li, 2000). In the early stages, late Mesozoic igneous rocks had calc-alkaline compositions that led some geologists to propose a compressional regime related to the subduction of paleo-Pacific plate, which continued until Late Cretaceous time (Jahn et al., 1990; Charvet et al., 1994; Lapierre et al., 1997), when bimodal volcanic rocks and associated A-type granites were emplaced in the coastal region (e.g., Martin et al., 1994; Qiu et al., 2004). However, a geological review of rift basins indicates that late Mesozoic tectonic regimes in Southeast China were extensional, perhaps analogous to the Basin and Range in North America, considered to result from lithospheric extension, which occurred concurrently with paleo-Pacific subduction (Gilder et al., 1991, 1996). In general, mafic dikes are the expression of extensional tectonics and mantle-derived magma generation (e.g., Hall, 1982; Hall and Fahrig, 1987; Ernst and Buchan, 2001). With this in mind, the mafic dikes of Southeast China can provide important information to understand the geodynamic evolution of this region (Li and McCulloch, 1998). As mentioned above, the occurrences of late Mesozoic mafic dikes in southern Jiangxi demonstrate that this region was dominated by lithospheric

extension. Such continental extension-related magmatism, although carrying subduction geochemical fingerprints, is not unusual in many orogen systems (e.g., Romer et al., 2001; Yang et al., 2004).

The following lines of evidence support the contention that all of Southeast China was dominated by extensional tectonics in the late Mesozoic.

1. Except for Late Cretaceous bimodal rocks, which are widely distributed in the coastal areas of Zhejiang, Fujian, and Guangdong provinces, abundant Jurassic bimodal volcanic rocks have been found in several localities in interior regions of Southeast China during recent geological surveys (Xing et al., 2004). Examples include: (a) the Fankeng Formation (Rb-Sr isochron age, 179 Ma) in southwestern Fujian, composed of tholeiites, which directly overlies plagiorhyolites; and (b) the Changpu Formation (Rb-Sr isochron age, 173–178 Ma) in southern Jiangxi, which consists of tholeiites and rhyolites, with A-type signatures (Chen et al., 2002; Xing et al., 2004). In addition, the thickness of the basalts in Jurassic bimodal volcanic rocks is equivalent to or larger than that of rhyolites, as shown by the Changpu Formation, Xunwu Country, in southern Jiangxi, which comprises 70% basalt and about 30% rhyolite, combining to form a suite of bimodal volcanic rocks (Chen et al., 2002).

2. Jurassic to Late Cretaceous A-type granites and alkaline rocks are present not only in the coastal regions of Southeast China (Qiu et al., 2004)—e.g., the Kuiqi peralkaline granite (93 ± 1Ma, Rb-Sr isochron age; Martin et al., 1994)—but also in interior regions of Southeast China (Li, 2000), such as the minor Middle–Late Jurassic A-type granite and alkali syenite that occur in southern Jiangxi; these include the Zhaibei A-type granite (171.6 ± 4.6 Ma, zircon SHRIMP U-Pb; Li et al., 2003), the Doutou A-type granite (178 Ma, Rb-Sr isochron dating of whole rock; Chen et al., 2002), and the Quannan alkali syenite (164.6 ± 2.8Ma, zircon SHRIMP U-Pb; Li et al., 2003). Hornblende from the Yangmei, Noumiao, and Tong'an syenite plutons in eastern Gangxi, and the Ma-Shan pluton in western Guangdong, yielded plateau ages of 161.6 ± 0.9 Ma, 161.0 ± 0.9 Ma, 163.2 ± 0.9 Ma, and 163.6 ± 2.0 Ma, respectively (Li et al, 2004). In addition, ^{40}Ar-^{39}Ar dating of hornblende for the Ejinao nepheline syenite and zircon U-Pb isotopic dating of the A-type Nankunshan granite in Southeast China yielded plateau ages of 127.5 ± 1.2 Ma (Zhou et al., 1996) and 147 ± 0.8 Ma (Liu et al., 2005), respectively. Highly precise zircon U-Pb dating of Mesozoic igneous rocks in Hong Kong shows that granitoids with A-type characteristics were intruded in this region in two periods, 164.4–159.9 Ma and 140 Ma (Davis et al., 1997; Sewell and Campbell, 1997).

3. In general, Middle Jurassic basalts and gabbros are mainly distributed in the interior regions of Southeast China, whereas Cretaceous basalts and gabbros are found in the coastal regions, showing a time-space zonation of igneous activity (see below). Geochemical studies show that the basaltic magmatism occurred in an extensional regime (Dong et al., 1997; Xu et al., 1999; Wang, 2002; Li et al., 2003, 2004; Xing et al., 2004; Xie et al., 2005a).

4. Cretaceous high-K calc-alkaline intrusive and volcanic rocks in Southeast China exhibit geochemical features similar to those formed in continental backarc and post-collision settings (Pirajno and Bagas, 2002) and were most likely formed in an extensional environment (Li, 2000; Wu et al., 2005). In addition, petrologic and geochemical characteristics of a Middle Jurassic granodiorite-diorite association that occurred in the interior region of Southeast China suggest that these rocks were formed by asthenospheric upwelling and lithospheric extension (Wang et al., 2003).

5. Beginning in the middle Mesozoic, rifting and basin formation commenced along the entire eastern margin of China (Gilder et al., 1991); granitoids with anomalously high REE and low T_{DM} model ages are distributed along NE-trending belts, and are related to juvenile mantle contributions and Mesozoic crust extension in Southeast China (Gilder et al., 1996;Chen and Jahn, 1998).

6. Most Cretaceous basins in Southeast China contain red clastic rocks associated with marl, gypsum, and evaporites, locally interlayered with basaltic and andesitic rocks, with similar characteristics to back-arc basins (Zhou and Li, 2000).

7. Studies of mafic dikes in northern Guangdong, Fuijian, and the islands of Chinmen and Liehyu indicate that tectonic regimes in this region were extensional rather than compressional one during the late Mesozoic (Lan et al., 1995; Li and McCulloch, 1998; Lee et al., 1998; Chen et al., 2000; Zhao et al., 2004).

8. Structural and radiometric reappraisal of the Wugongshan massif in the western part of Jiangxi Province suggests a Late Triassic age for ductile deformation and an Early Cretaceous age for the final doming, similar to a metamorphic core

complex formed in an extensional tectonic regime (Faure et al., 1996).

9. Statistical studies of the timing of Mesozoic mineralization in Southeast China indicate that three pulses of large-scale mineralization took place, namely 170–150 Ma, 140–125 Ma, and 110–80 Ma, corresponding to a multi-stage lithospheric extension of the southeast margin of Eurasia (Mao et al., 2004).

Taking into consideration the distribution of extension-related igneous rocks, it is probable that lithospheric extension occurred in interior regions of Southeast China in Middle to Late Jurassic time, corresponding to a regional extension of all of Southeast China during the Cretaceous (Xie et al., 2005a, 2005b). Lithospheric extension was episodic rather than continuous between the Jurassic and Cretaceous periods. For example, three stages of bimodal igneous rocks are recognized, including 170 Ma, 154–121 Ma, and 115–85 Ma (Xing et al., 2004), as well as reliable isotope age data which indicate that Mesozoic high-K I-type and A-type granites in Southeast China formed during four major episodes, at 136–146 Ma, 122–129 Ma, 101–109 Ma, and 87–97 Ma (Li, 2000). Therefore, intermittent lithospheric extension probably occurred during different episodes, although the precise timing of extension remains to be further studied.

Geodynamic setting

Although lithospheric extension was dominant in Southeast China during the late Mesozoic period, several lines of evidence indicate that subduction of the paleo-Pacific plate played an important role in the geodynamic evolution of the area, especially between Late Jurassic and Cretaceous time. For example, a distinct southeastward younging trend is apparent for Mesozoic magmatism, from Middle Jurassic (180–160 Ma) granitoids in the eastern Wuyi Mountain, to Late Jurassic–Early Cretaceous (160–140 Ma) granitoids and volcanic rocks, between Wuyi and Daiyun Mountain, to Cretaceous granitoids and volcanic rocks along the coastal areas (Figs. 1 and 2 of Zhou and Li, 2000; Qiu et al., 2004). In addition, late Mesozoic magmatic belts in Southeast China are aligned along NE trends (Zhou and Li, 2000), approximately parallel to the subduction zone (Maruyama, 1997). Moreover, Late Jurassic to Cretaceous basaltic magmatism shows island-arc magma signatures, as exemplified by Nb and Ta negative anomalies shown in Figure 7 (Charvet et al., 1994; Lan et al., 1995; Lapierre et al., 1997; Lee et al., 1998; Chen et al., 2000; Xie et al., 2001; Xiong et al., 2003; Li et al., 2004; Zhao et al., 2004; this study). All these features indicate a possible relationship between late Mesozoic igneous provinces in Southeast China and subduction of the Paleo-Pacific plate (Northrup et al., 1995). This view is also supported by recent seismic tomographic images in East Asia (Kárason and van der Hilst, 2000) and the development of late Mesozoic accretionary complexes along the Asian continental margin (Maruyama, 1997; Zyabrev and Matsuoka, 1999). Therefore, lithospheric extension during Late Jurassic and Cretaceous time could have resulted from backarc extension, probably induced by slab roll-back during paleo-Pacific subduction.

However, the Middle Jurassic granite-gabbro or rhyolite-basalt bimodal suites as well as A-type granites and syenite are mainly distributed along east-west belts in interior Southeast China, such as southern Jiangxi. The basaltic rocks show intraplate magma geochemical characteristics rather than island-arc signatures (Chen et al., 2002; Li et al., 2003, 2004; Wang et al., 2005; Xie et al., 2005a). However, Jurassic extension-related magmatism has not been found in the coastal region of Southeast China thus far. In addition, the Indosinian continental orogenic event was dominated by the development of thrust-and-nappe tectonics until the end of the Early Jurassic (J_1) (Chen, 1999). All of these features suggest that lithospheric extension in Southeast China probably resulted from post-Indosinian orogenic collapse rather than being related to subduction of the paleo-Pacific plate in the Middle Jurassic (Li et al., 2004). Paleontological studies indicated that subduction-accretion events along the eastern margin of the Eurasian plate took place in the Late Jurassic (Zyabrev and Matsuoka, 1999). Therefore, lithospheric extension probably resulted from post-orogenic collapse during the Middle Jurassic period.

Implication for lithospheric thinning

Studies of mantle-derived xenoliths suggest that ancient lithospheric mantle was removed and replaced by thinner, hotter, more fertile mantle material, during late Mesozoic to Cenozoic time in Southeast China (Xu et al., 2000, 2002; Zheng et al., 2004). However, this replacement may not be complete throughout the region, resulting in the presence of old lithospheric relics in the uppermost layers of the mantle (Xu et al., 2002). Geochemical and isotopic characteristics of Cretaceous basaltic

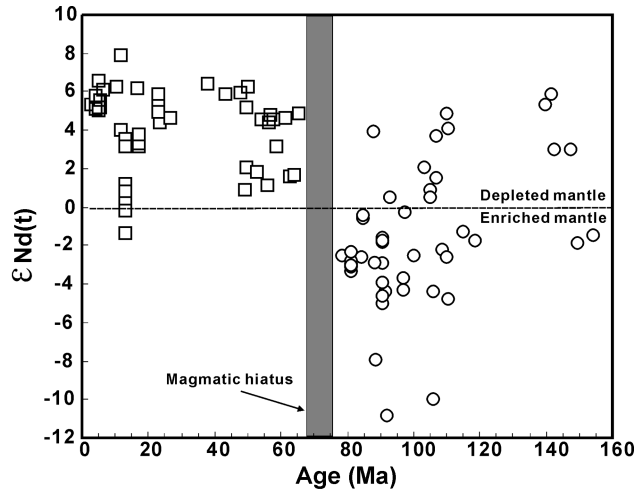

FIG. 13. Temporal variations in the Nd isotopic composition of basaltic magmatism in Southeast China. The shaded area highlights the period during which no magmatism has been observed thus far in this region. Data sources: Peng et al. (1986), Li (1990), Lan et al. (1995), Lapierre et al. (1997), Lee et al. (1998), Li and McCulloch (1998), Chen et al. (2000), Zou et al. (2000), Xie et al. (2001), Ho et al. (2003), Xiong et al. (2003), Zhu et al. (2004), Li et al (2004), Xie et al. (2005c).

rocks are significantly different from those for Cenozoic basalts and the secular magma source responsible for Cretaceous and Cenozoic basaltic magmatism changed from the subduction-modified lithospheric mantle to ascending asthenospheric mantle magmatism (Chung et al., 1997; Yu et al., 2003; Xie et al., 2005b; this study). All these features indicated that lithospheric replacement and thinning did occur in Southeast China. Nevertheless, the timing and mechanisms for this event remain poorly understood.

Geochemical characteristics for late Mesozoic to Cenozoic basaltic rock could provide information on the temporal variation of magma generation and evolution of the lithospheric mantle, especially the $\varepsilon_{Nd}(T)$ value for basaltic rock, because the $\varepsilon_{Nd}(T)$ values are not affected by not only secondary alternation but also magmatic processes such as fractional crystallization and partial melting (cf. Rollinson, 1993). Consequently, the variations in $\varepsilon_{Nd}(T)$ for mantle-derived magmas can provide important information on lithospheric thinning (e.g., Perry et al., 1988; Daley and DePaolo, 1992; DePaolo and Daley, 2000). To gain a better understanding of the relationship of changing magma sources and lithospheric thinning, geochemical and isotopic data from this study integrated with published data of Mesozoic and Cenozoic basaltic magmatism provide constraints on lithospheric thinning beneath the crust in Southeast China. As discussed previously, the studied mafic dikes were not significantly affected by crustal contamination. In addition, crustal contamination was insignificant in the petrogenesis of late Mesozoic and Cenozoic basalts (e.g., Zou et al., 2000; Xie et al., 2001). Therefore, the isotopic variation in magmas, as illustrated in Figure 13, reflects mantle sources that were changing with time. From Late Jurassic to Late Cretaceous, the $\varepsilon_{Nd}(T)$ values for basaltic rocks in Southeast China have gradually decreased, indicating that the contribution from the subduction-modified enriched mantle increased with time in this region . However, Cenozoic basalts show an increase of the ε_{Nd} (T) values with time, although they mainly originated from a depleted asthenospheric mantle. Moreover, Cretaceous and Cenozoic basaltic rocks with different source characters were separated by an important hiatus (80–65 Ma), when the sudden cessation of extensive Mesozoic magmatism occurred, heralding an important change of geodynamic regime in Southeast China (Li, 2000).

DePaolo and Daley (2000) proposed that the depth of the lithosphere-asthenosphere boundary can be inferred from the ε_{Nd} and $^{87}Sr/^{86}Sr$ of the lavas as a function of age, and an estimate of the depth of the magma source can be obtained on the

basis of its silica saturation. From Figures 8, 11, and 12, Upper Jurassic to Cretaceous basaltic rocks have higher $^{87}Sr/^{86}Sr$ and lower $^{143}Nd/^{144}Nd$ values than Upper Cenozoic basalts, which indicates that subcontinental lithosphere mantle beneath the Cathaysia block had gradually evolved from enriched lithospheric mantle in the Cretaceous to depleted asthenospheric mantle in the Late Cenozoic (e.g. Xie et al., 2005c). This temporal shift, from a lithospheric to asthenospheric magma source beneath the Cathaysia block, is similar to that seen in the Basin and Range province in the United States, in northeast Japan, the Rio Grande rift, and in the North China Carton (NCC) (e.g., Perry et al., 1988; Tatsumi et al., 1988; Nohda et al., 1988; Fitton et al., 1991; Daley and DePaolo., 1992; Leeman and Harry, 1993; DePaolo and Daley, 2000; Xu, 2001; Xu et al., 2004), where involvement of subcontinental lithosphere as a magma source significantly decreased with time as lithosphere extension and thinning proceeded. Therefore, we suggest that involvement of the asthenospheric mantle beneath the crust in Southeast China gradually increased with time, and the temporal shift from a lithospheric to asthenospheric magma source was probably related to progressive lithospheric extension and thinning as well as asthenospheric upwelling (Chung et al., 1997; Xu et al., 2000; Wang and O'Reilly, 2003).

If this interpretation is correct, mantle-derived magmas with different geochemical characteristics can provide important information on lithospheric thinning. In our present state of knowledge, late Mesozoic basaltic magmatism, such as 154–149 Ma high-Mg basaltic rocks from southern Hunan Province, mainly originated from the enriched lithospheric mantle that melted due to thinning (Li et al., 2004) since the Late Jurassic when lithospheric thinning probably started in Southeast China, and continued at least until the end of the Late Cretaceous. This is supported by the fact that Paleocene basaltic rocks in this region do not exhibit geochemical and isotopic affinities with OIB (Xie et al., 2005c). Most recently, compilation of a large number of available precise ages in eastern China indicates that 132–120 Ma was the most important period of igneous activity, corresponding to the most intense period of lithospheric thinning (Xu et al., 2004; Wu et al., 2005). It can be seen from Figure 12 that the shift from lithosphere-derived (Cretaceous) to asthenosphere-derived (Cenozoic) partial melts in Southeast China is attributable to thinning of the lithosphere, and this scenario is similar to the late Mesozoic large Antarctic Peninsula igneous province where lithospheric thinning was a consequence of voluminous silicic volcanism in the Middle Jurassic, coupled with regional extension (e.g., Riley et al., 2003). Therefore, the lithospheric thinning beneath the crust most likely took place during the Jurassic to Cretaceous period and was genetically associated with the late Mesozoic large igneous province in Southeast China; this was accompanied by a mantle source shift for basaltic magmatism during lithospheric extension.

Conclusions

K-Ar dating indicates that the mafic dikes in southern Jiangxi Province were emplaced in the Late Jurassic to Cretaceous (147–79 Ma) time and that these dikes are dominantly subalkaline in composition, with lesser components in the alkali series. Major- and trace-element geochemistry and isotopic systematics demonstrate that melts were dominated by an enriched lithospheric (EM2) mantle component, mixed with different minor proportions of depleted mantle. Southeast China was dominated by episodic lithospheric extension during the late Mesozoic. Lithospheric extension in the interior regions was related to post-orogenic collapse in the Middle Jurassic, whereas regional extension throughout southeast China was probably related to paleo-Pacific subduction during the Cretaceous. Lithospheric thinning continued until the end of the Late Cretaceous and was genetically associated with the late Mesozoic large igneous province in Southeast China, accompanied by a mantle source shift for late Mesozoic basaltic magmatism in this region.

Acknowledgments

Profs. Xin-Ming Zhou and Xian-Hua Li are acknowledged for insightful discussions and help at various stages of this study. Song-Rong Li, Liang Qi, Yin Liu, Wei Chen, Da-Guan Yu, Tai-Yang Guang, and Chun-Gen Liu are thanked for their assistance in the laboratory and field trips. This study was jointly supported by the National Science Foundation of China (40402011 and 40434011), the State Key Laboratory of Geological Processess and Mineral Resources, China University of Geosciences (GPM40504), State Key Laboratory of Ore Deposit Geochemistry, Institute of Geochemistry, Chinese Academy of Sciences (200402), the Chinese Acad-

emy of Sciences (KZCX3-SW-125), and the China Postdoctoral Science Foundation. Franco Pirajno publishes with the permission of the Director of the Geological Survey of Western Australia.

REFERENCES

BGMR (Bureau of Geology and Mineral Resources of Jiangxi Province), 1984, Regional geology of Jiangxi province: Beijing, China, Geological Publishing House, 921 p. (in Chinese with English abstract).

Charvet, J., Lapierre, H., and Yu, Y., 1994, Geodynamic significance of the Mesozoic volcanism of southeastern China: Journal of Southeast Asia Earth Sciences, v. 9, p. 387–396.

Chen, A., 1999, Mirror-image thrusting in the South China orogenic belt: Tectonic evidence from western Fujian, southwestern China: Tectonophysics, v. 305, p. 497–519.

Chen, C.-H., Lin, W., Lu, H.-Y., Lee, C.-Y., Tien, J.-L., and Lai, Y.-H., 2000, Cretaceous fractionated I-type granitoids and metaluminous A-type granites in SE China: The late Yanshanian post-orogenic magmatsim: Transactions of the Royal Society of Edinburgh: Earth Sciences, v. 91, p. 195–205.

Chen, J. F., and Jahn, B. M., 1998, Crustal evolution of southeastern China: Nd and Sr isotopic evidence: Tectonophysics, v. 284, p. 101–133.

Chen, P. R., Hua, R. M., Zhang, B. T., Liu, J. J., and Fan, C. F., 2002, Early Yanshanian post-orogenic granitoids in the Nanling region-petrological constraints and geodynamic settings: Science in China (D), v. 45, p. 755–768.

Chung, S. L., Cheng, H., Jahn, B. M., O'Reilly, S. Y., and Zhu, B.-Q., 1997, Major and trace, and Sr-Nd isotope constrains on the origin of Paleogene volcanism in South China prior to the South China Sea opening: Lithos, v. 40, p. 203–220.

Chung, S.L., Jahn, B. M., Chen, S. J., Lee, T., and Chen, C.-H., 1995, Miocene basalts in northwestern Taiwan: Evidence for EM-type sources in the continental lithosphere: Geochimica et Cosmichimica Acta, v. 59, p. 549–555.

Chung, S. L., Sun, S.-S., Tu, K., Chen, C.-H., and Lee, C. Y., 1994, Late Cenozoic basaltic volcanism around the Taiwan Strait, SE China: Product of lithosphere-asthenosphere interaction during continental extension: Chemical Geology, v. 112, p. l—20.

Collins, W. J., 2002, Nature of extensional accretionary orogens: Tectonics, v. 21 [10.1029/2000TC001272].

Daley, E. E., and DePaolo, D. J., 1992, Isotopic evidence for lithospheric thinning during extension: Southeastern Great Basin: Geology, v. 20, p. 104–108

Davis, D. W., Sewell, R. J., and Campbell, S. D. G., 1997, U-Pb dating of Mesozoic igneous rocks from Hong Kong: Journal of the Geological Society of London, v. 154, p. 1067–1076.

DePaolo, D. J., and Daley, E. E., 2000, Neodymium isotopes in basalts of the southwest Basin and Range and lithospheric thinning during continental extension: Chemical Geology, v. 169, p. 157–185.

Dong, C. W., Zhou, X. M., and Li, H. M., 1997, Late Mesozoic crust/mantle interaction in southeastern Fujian: Isotopic evidence from the Pingtan igneous complex: Chinese Science Bulletin, v. 42, p. 495–498.

Dupuy, C., Liotard, J. M., and Dostal, J., 1992, Zr/Hf fractionation in intraplate basaltic rocks: Carbonate metasomatism in the mantle source: Geochimica et Cosmochimica Acta, v. 56, p. 2417–2423.

Ernst, R. E., and Buchan, K. L., 2001, The use of mafic dike swarms in identifying and locating mantle plumes: Geological Society of America, Special Paper, v. 352, p. 247–266.

Faure, M., Sun, Y., Shu, L., Monié, P., and Charvet, J., 1996, Extensional tectonics within a subduction-type orogen. The case study of the Wugongshan dome (Jiangxi Province, southeastern China): Tectonophysics, v. 263, p. 77–106.

Fitton, J. G., James, D., and Leeman, W. P., 1991, Basic magmatism associated with Late Cenozoic extension in the western United States: Compositional variations in space and time: Journal of Geophysical Research (B), v. 96, p. 13,693–13,711.

Flower, M. F. J., Zhang, M., Chen, C.-Y., Tu, K., and Xie, G. H., 1992,Magmatism in the South China Basin, 2. Post-spreading Quaternary basalts from Hainan Island, south China: Chemical Geology, v. 97, p. 65–87.

Furman, T., and Graham, D., 1999, Erosion of lithospheric mantle beneath the East African Rift system: Geochemical evidence from the Kivu volcanic province: Lithos, v. 48, p. 237–262.

Gao, S., Luo, T.-C., Zhang, B.-R., Zhang, H.-F., Han, Y.-W., Zhao, Z.-D., and Hu, Y.-K., 1998, Chemical composition of the continental crust as revealed by studies in East China: Geochimica et Cosmochimica Acta, v. 62, p. 1959–1975.

Gilder, S. A., Gill, J., Coe, R. S., Zhao, X. X., Liu, Z. W., and Wang, G. X., 1996, Isotopic and plaeomagnetic constraints on the Mesozoic tectonic evolution of South China: Journal of Geophysical of Research(B), v. 107, p. 16137–16154.

Gilder, S. A., Keller, G. R., Luo, M., and Goodell, P. C., 1991, Timing and spatial distribution of rifting in China: Tectonophysics, v. 197, p. 225–243.

Griffin, W. L., Wang, X., Jackson, S. E., Pearson, N. J., O'Reilly, S. Y., Xu, X., and Zhou, X., 2002, Zircon chemistry and magma mixing, SE China: In-situ analysis of Hf isotopes, Tonglu and Pingtan igneous complexes: Lithos, v. 61, p. 237–269.

Hall, H. C., 1982, The importance and potential of mafic dyke swarm in studies of geodynamic process: Geosciences Canada, v. 9, p. 145–154.

Hall, H. C., and Fahrig, W. F., 1987, Mafic dyke swarms: Geological Association of Canada Special Paper, v. 34, 503 p.

Ho, K. S., Chen, J. C., Lo, C. H., and Zhao, H.-L., 2003, ^{40}Ar-^{39}Ar dating and geochemical characteristics of late Cenozoic basaltic rocks from the Zhejiang–Fujian region, SE China: Eruption ages, magma evolution, and petrogenesis: Chemical Geology, v. 197, p. 287–318.

Ho, K. S., Chen, J. C., Smith, A. D., and Juang, W. S., 2000, Petrogenesis of two groups of pyroxenite from Tungchihsu, Penghu Islands, Taiwan Strait: Implications for mantle metasomatism beneath SE China: Chemical Geology, v. 167, p. 355–372.

Hu, S. B., He, L. J., and Wang, J. Y., 2000, Heat flow in the continental area of China, a new data set: Earth and Planetary Science Letters, v. 179, p. 407–419.

Irvine, T. N., and Baragar, W. R. A., 1971, A guide to the chemical classification of the common volcanic rocks: Canadian Journal of Earth Science, v. 8, p. 523–548.

Jahn, B. M., 1986, Mid-ocean ridge or marginal basin origin of the East Taiwan Ophiolite: Chemical and isotopic evidence: Contributions to Mineralogy and Petrology, v. 92, p. 194–206.

Jahn, B. M., Zhou, X. H., and Li, J. L., 1990, Formation and tectonic evolution of southeastern China and Taiwan: Isotopic and geochemical constraints: Tectonophysics, v. 183, p. 145–160.

Jochum, K. P., McDonough, W. F., Palme, H., and Spettel, B., 1989, Compositional constraints on the continental lithospheric mantle from trace elements in spinel peridotite xenoliths: Nature, v. 340, p. 548–550.

Kárason, H., and van der Hilst, R., 2000, Constraints on mantle convection from seismic tomography: Geophysics Monographs, v. 121, p. 277–288.

Lan, C. Y., Chung, S. L., Mertzman, S. A., and Chen, C, H., 1995, Mafic dikes from Chinmen and Liehyu islands off SE China, petrochemical characteristics and tectonic implication: Journal of the Geological Society of China, v. 38, p. 183–214.

Lapierre, H., Jahn, B. M.,Charver, J., and Yu, Y. W. ,1997, Mesozoic felsic arc magmastism and continental olivine tholeiites in Zhejing province and their relationship with the tectonic activity in southeastern China: Tectonophysics, v. 274, p. 321–338.

Le Maitre, R. W., Bateman, P., Dudek, A., Keller, J., Le Bas, M. J. L., Sabine, P. A., Schmid, R., Sorensen, H., Sktreckeisien, A., Woodley, A. R., and Zanettin, B., 1989, A classification of igneous rocks and glossary of terms: Oxford, UK, Blackwell Scientific Publications, 193 p.

Lee, C. Y., Chung, S. L., Chen, C. H., Lin, W., Lo, C. H., Jahn, B. M., and Li, X., 1998, Petrochemical characteristics of mafic dikes from the Fujian area: Mantle evolution and tectonic implication of SE China since the Late Mesozoic: EOS (Transactions of the American Geophysical Union), v. 79, no. 24, p. W124–125.

Leeman, W. P., and Harry, D. L., 1993, A binary source model for extension-related magmatism in the Great basin, west North America: Science, v. 262, p. 1550–1554.

Li, J.-W., Zhou, M.-F., Li, X.-F., Fu, Z.-R., and Lia, Z.-J., 2001, The Hunan-Jiangxi strike-slip fault system in southern China, southern termination of the Tan-Lu fault: Journal of Geodynamics, v. 32, p. 333–354.

Li, X. H., 1990. Discussion of the genesis of middle and mafic dikes from the Zhuguanghan rock body: Evidence from Sr, Nd, and O isotopes: Chinese Science Bulletin, v. 35, p. 1247–1249 (in Chinese).

Li, X. H., 2000, Cretaceous magmatism and lithospheric extension in Southeast China: Journal of Asian Earth Sciences, v.18, p. 293–305.

Li, X.-H., Chen, Z. G., Liu, D. Y., and Li, W. X., 2003, Jurassic gabbro-granite-syenite suites from southern Jiangxi province, SE China: Age, origin, and tectonic significance: International Geological Review, v. 45, p. 898–921.

Li, X. H., Chung, S. L., Zhou, H. W., Lo, C. H., Liu, Y., and Chen, C. H., 2004, Jurassic intraplate magmatism in southeastern Hunan-eastern Guangxi: $^{40}Ar/^{39}Ar$ dating, geochemistry, Sr-Nd isotopes, and implications for tectonic evolution of SE China, *in* Malpas, J., Fletcher, C., and Ali, J. R., eds., Tectonic process in the evolution of China: Geological Society of London Special Publication, v. 226, p. 193–215.

Li, X. H., and McCulloch, M. T., 1996, Secular variation in the Nd isotopic composition of Neoproterozoic sediments from the southern margin of the Yangtze block: Evidence for a Proterozoic continental collision in Southeast China: Precambrian Research, v. 76, p. 67–76.

Li, X. H., and McCulloch, M. T.,1998, Geochemical characteristics of Cretaceous mafic dikes from northern Guangdong, SE China: Age, origin, and tectonic significance, *in* Flower, M. F. J., Chung, S.-L., Lo, C.-H., and Lee, T. Y. eds., Mantle dynamics and plate interaction in East Asia: Washington, DC, American Geophysical Union: Geodynamics series, v. 27, p. 405–419.

Ling, H. F., Shen, W. Z., Deng, P., Jiang, S. Y., Jiang, Y. H., Ye, H. M., Pu, W., and Tan, Z, Z, 2005, Geochemical characteristics and genesis of the Luxi-Xianrenzhang diabase dikes in Xiazhuang uranium orefield, Northern Guangdong Province: Acta Geologica Sinica (English edition), v. 79, p. 497–506.

Liu, C. Q., Masuda, A., and Xie, G. H., 1994, Major- and trace- element compositions of Cenozoic basalts in eastern China: Petrogenesis and mantle source: Chemical Geology, v. 114, p. 19–42.

Liu, C. S., Chen, X. M., Wang, R. C., Zhang, W. L., and Hu, H., 2005, Isotopic dating and origin of complexly zoned micas for A-type Nankunshan aluminous gran-

ite: Geological Reviews, v. 51, p. 193–200 (in Chinese with English abstract).

Mao, J. W., Xie, G. Q., Li, X. F., Zhang, C. Q., and Mei, Y. X., 2004, Mesozoic large scale mineralization and multiple lithospheric extensions from South China: Earth Science Frontiers, v. 11, p. 45–56 (in Chinese with English abstract).

Martin, H., Bonin. B., Capdevila, R., Jahn, B. M., Lameyre, J., and Wang, Y., 1994, The Kuiqi peralkaline granitic complex (SE China): Petrology and geochemistry: Journal of Petrology, v. 35, p. 983–1015.

Maruyama, S., 1997, Pacific-type orogeny revised: Miyashiro-type orogeny proposed: The Island Arc, v. 6, p. 91–120.

McCulloch, M. T., and Gamble, T. A., 1991, Geochemical and geodynamical constraints on subduction zone magmatism: Earth and Planetary Science Letters, v. 102, p. 358–374.

Nohda, S., Tatsumi, Y., Otofuji, Y., Matsuda, T., and Ishizaka, K., 1988, Asthenospheric injection and back-arc opening: Isotopic evidence from the northeast Japan: Chemical Geology, v. 68, p. 317–327.

Northrup, C. J., Royden, L. H., and Burchfiel, B. C., 1995, Motion of the Pacific plate relative to Eurasia and its potential relation to Cenozoic extension along the eastern margin of Eurasia: Geology, v. 23, p. 719–722.

Peng, Z. C., Zartman, R. E., Futa, K., and Chen, D. G., 1986, Pb, Sr and Nd isotopic systematics and chemical characteristics of Cenozoic basalts, eastern China: Chemical Geology, v. 59, p. 3–33.

Perry, F. V., Baldridge, W. S., and DePaolo, D. J., 1988, Chemical and isotopic evidence for lithospheric thinning beneath the Rio Grande rift: Nature, v. 332, p. 432–434.

Piccirillo, E. E., Civetta, L., Petrini, R., Longinelli, A., Bellieni, G., Comin-Chiaramontl, P., Marques, L. S., and Melfi, A. J., 1989, Regional variations within the Paraná flood basalts (southern Brazil): Evidence for subcontinental mantle heterogeneity and crust contamination: Chemical Geology, v. 75, p. 103–122.

Pirajno, F., and Bagas, L., 2002, Gold and silver metallogeny of the South China fold belt: A consequence of multiple mineralizing events?: Ore Geology Reviews, v. 20, p. 109–126.

Qi, L., and Grégoire, D. C., 2000, Determination of trace elements in twenty-six Chinese geochemistry reference materials by inductively coupled plasma-mass spectrometry: Geostandard Newsletter, v. 24, p. 51–63.

Qi, Q., Taylor, L. A., and Zhou, X., 1994, Geochemistry and petrogenesis of three series of Cenozoic basalts from southeastern China: International Geology Review, v. 36, p. 435–451.

Qi, Q., Taylor, L. A., and Zhou, X.M., 1995, Petrology and geochemistry of mantle peridotite xenoliths from SE China: Journal of Petrology, v. 36, p. 55–79.

Qiu, J.-S.,Wang, D.-Z., McInnes, B. I., Jiang, S.-Y., Wang, R.-C., and Kanisawa, S., 2004, Two subgroups of A-type granites in the coastal area of Zhejiang and Fujian provinces, SE China: Age and geochemical constraints on their petrogenesis: Transactions of the Royal Society of Edinburgh: Earth Sciences, v. 95, p. 227–236.

Ren, J., Tamaki, K., Li, S., and Zhang, J., 2002, Late Mesozoic and Cenozoic rifting and its dynamic setting in Eastern China and adjacent areas: Tectonophysics, v. 344, p. 175–205.

Riley, T. R., Leat, P. T., Kellery, S. P., Millar, I. L., and Thirlwall, M. F., 2003, Thinning of the Antarctic Peninsula lithosphere thought the Mesozoic: Evidence from Middle Jurassic basaltic lavas: Lithos, v. 67, p. 163–179.

Rock, N. M. S., Bowes, D. R., and Wright, A . E., 1990, Lamprophyres: Glasgow and London, UK, Blackie, 156 p.

Rollinson, H. R., 1993, Using geochemical data: Evaluation, presentation, interpretation: New York, NY, Longman Scientific and Technical, 353 p.

Romer, R. L., Förster, H. J., and Breitkreuz, C., 2001, Intracontinental extensional magmatism with a subduction fingerprint: The late Carboniferous Halle Volcanic Complex: Contributions to Mineralogy and Petrology, v. 141, p. 201–221.

Rudnick, R. L., McDonough, W. F., and Chapell, B. W., 1993, Carbonatite metasomatism in the northern Tanzanian mantle: Petrographic and geochemical characteristics: Earth and Planetary Science Letters, v. 114, p. 463–475.

Sewell, R. J., and Campbell, S. D. G., 1997, Geochemistry of coeval Mesozoic plutonic and volcanic suites in Hong Kong: Journal of the Geological Society of London, v. 154, p. 1053–1066.

Sun, S. S., and McDonough, W., 1989, Chemical and isotopic systematic basalt: Implication for mantle composition and processes. *in* Saunders, A .D., and Norry, M. J., eds., Magmatism in the ocean basins: Geological Society of London Special Publication, v. 42, p. 313–345.

Tanaka, T., Togashi, S., Kamioka, H., Amakawa, H., Kagami, H., Hamamoto, T., Yuhara, M., Orihashi, Y., Yoneda, S., Shimizu, H., Kunimaru, T., Takahashi, K., Yanagi, T., Nakano, T., Fujimaki, H., Shinjo, R., Asahara, Y., Tanimizu, M., and Dragusanu, C., 2000, Jndi-1: A neodymium isotopic reference in consistency with LaJolla neodymium: Chemical Geology, v.168, p. 279–281.

Tatsumi, Y., Nohda, S., and Ishizaka, K., 1988, Secular variation of magma source compositions beneath the northeast Japan arc: Chemical Geology, v. 68, p. 309–316.

Tu, K., Flower, M. F. J., Carlson, R. W., Xie, G. H., Chen, C. Y., and Zhang, M., 1992, Magmatism in the South China Basin: 1. Isotopic and trace element evidence

for an endogenous Dupal mantle component: Chemical Geology, v. 97, p. 47–63.

Tu, K., Flower, M. F. J., Carlson, R. W., Zhang, M., and Xie, G. H., 1991, Sr, Nd, and Pb isotopic compositions of Hainan basalts (South China): Implications for a subcontinental lithosphere Dupal source: Geology, v. 19, p. 567–569.

Wang, K. L., and O'Reilly, S. Y., 2003, Proterozoic mantle lithosphere beneath the extended margin of the South China block: In situ Re-Os evidence: Geology, v . 31, p. 709–712.

Wang, Y. J., Fan, W. M., Guo, F., Peng, T. P., and Lin, G., 2003, Geochemistry of early Mesozoic potassium-rich diorites-granodiorites in southeastern Hunan Province, South China: Petrogenesis and tectonic implications: Geochemical Journal, v. 37, p. 427–448.

Wang, Y. J., Fan, W. M., Peng, T. P., and Guo, F., 2005, Elemental and Sr–Nd isotopic systematics of the early Mesozoic volcanic sequence in southern Jiangxi Province, South China: Petrogenesis and tectonic implications: International Journal of Earth Sciences, v. 94, p. 53–65.

Wang, Z., 2002, The origin of the Cretaceous gabbro in the Fujian coastal region of SE China: Implications for deformations-accompanied magmatism: Contributions to Mineralogy and Petrology, v. 144, p. 230–240.

Wilson, M., 1989, Igneous prtrogenesis: London, UK, Unwin Hyman, 466 p.

Wu, F.-Y., Lin, J.-Q., Wilde, S. A., Zhang X. O., and Yang, J.-H., 2005, Nature and significance of the Early Cretaceous giant igneous event in eastern China: Earth and Planetary Science Letters, v. 233, p. 103–119.

Xie, G. Q., Mao, J. W., Hu, R. Z., 2005a, Jurassic intraplate basaltic magmatism in Southeast China: Evidence from geological and geochemical characteristics of the Chebu gabbroite in southern Jiangxi province: Acta Geologica Sinica (English edition), v. 79, p. 662–672.

Xie, G. Q.,Mao, J. W., Hu, R. Z., Li, R. L., and Cao, J. J., 2005b, Discussion of some problems of Mesozoic and Cenozoic geodynamics in Southeast China: Geological Review, v. 51, p. 613–620 (in Chinese with English abstract).

Xie, G. Q., Mao, J. W., Hu, R. Z., Li, R. L., and Cao, J. J., 2005c, Secular evolution of Cretaceous–Cenozoic lithosphere mantle beneath the Cathaysia block: Geochemical evidence for temporal variations in basaltic magmatism: Geochimica et Cosmochimica Acta, v. 69 (suppl.), p. A109.

Xie, X., Xu, X. S., Zou, H. B., and Xing, G. F., 2001,Trace element and Nd-Sr-Pb isotope studies of Mesozoic and Cenozoic basalts in coastal areas of SE China: Acta Petrologica Sinica, v. 17, p. 617–628 (in Chinese with English abstract).

Xing, G. F., Yang, Z. L., Chen, R., Shen, J. L., Wei, N. Y., and Zhou, Y. Z., 2004, Three stages of Mesozoic bimodal igneous rocks and their tectonic implications on the continental margin of southeastern China: Acta Geologica Sinica (English edition), v. 78, p. 27–39.

Xiong, X. -L., Li, X. -H., Xu, J. -F., Li, W.-X., Zhao, Z.-H., Wang, Q., and Chen, X.-M., 2003, Extremely high-Na adakite-like magmas derived from alkali-rich basaltic underplate: The Late Cretaceous Zhangtang andesites in the Huichang basin, SE China: Geochemical Journal, v. 37, p. 233–252.

Xu, X., Dong, C., Li, W., and Zhou, X., 1999, Late Mesozoic intrusive complexes in the coastal area of Fujian, SE China: The significance of the gabbro-diorite-granite association: Lithos, v. 46, p. 299–315.

Xu, X., O'Reilly, S. Y., Griffin, W. L., Deng, P., and Pearson, N. J., 2005, Relict Proterozoic basement in the Nanling Mountains (SE China) and its tectonothermal overprinting: Tectonics, v. 24, TC2003 [doi: 10.1029 / 2004 TC001652].

Xu, X. S., O'Reilly, S. Y., Griffin, W. L., and Zhou, X .M., 2000, Genesis of young lithospheric mantle in SE China: Journal of Petrology, v. 41, p. 111–148.

Xu, X. S., O'Reilly, S. Y., Griffin, W. L., and Zhou, X. M., 2003. Enrichment of upper mantle peridotite: Petrological, trace element, and isotopic evidence in xenoliths from SE China: Chemical Geology, v. 198, p. 163–188.

Xu, Y. G., 2001, Thermo-tectonic destruction of the Archean lithospheric keel beneath eastern China: Evidence, timing, and mechanism: Physics and Chemistry of the Earth (A), v. 26, p. 747–757.

Xu, Y. G., Huang, X. L., Ma, J. L., Wang, Y. B., Iizuka, Y., Xu, J. F., Wang, Q., and Wu, X. Y., 2004, Crust-mantle interaction during the thermo-tectonic reactivation of the North China Carton: SHRIMP zircon U–Pb age, petrology, and geochemistry of Mesozoic plutons in western Shandong: Contributions to Mineralogy and Petrology, v. 147, p. 750–767.

Xu, Y. G., Sun, M., Yan, W., Liu, Y., Huang, X. L., and Chen, X. M., 2002, Xenolith evidence for polybaric melting and stratification of the upper mantle beneath South China: Journal of Asian Earth Sciences, v. 20, p. 937–954.

Yang, J.-H., Chung, S.-L., Zhai, M.-G., and Zhou, X.-H., 2004, Geochemical and Sr-Nd-Pb isotopic compositions of mafic dikes from the Jiaodong Peninsula, China: Evidence for vein-plus-peridotite melting in the lithospheric mantle: Lithos, v. 73, p. 145–160.

Yang, W., 2003, Flat mantle reflectors in Eastern China: Possible evidence of lithospheric thinning: Tectonophysics, v. 369, p. 219–230.

Yu, J. H., Xu, X. S., O'Reilly, S. Y., Griffin, W. L., and Zhang, M., 2003, Granulite xenoliths from Cenozoic Basalts in SE China provide geochemical fingerprints to distinguish lower crust terranes from the North and South China tectonic blocks: Lithos, v. 67, p. 77–102.

Zhang, Z., Badal, J., Li, Y., Chen, Y., Yang, L., and Teng, J., 2005, Crust-upper mantle seismic velocity struc-

ture across Southeastern China: Tectonophysics, v. 395, p. 137–157.

Zhao, J. H., Hu, R. Z., and Liu, S., 2004, Geochemistry, petrogenesis, and tectonic significance of Mesozoic mafic dikes, southeastern China: International Geology Review, v. 46, p. 542–557.

Zheng, J., O'Reilly, S. Y., Griffin, W. L., Zhang, M., Lu, F. X., and Liu, G. L., 2004, Nature and evolution of Mesozoic–Cenozoic lithospheric mantle beneath the Cathaysia block, SE China: Lithos, v. 74, p. 41–65.

Zhou, L. D., Zhao, Z. H., and Zhou, G. F., 1996, Isotopic chronology of some alkaline rock bodies in China: Geochimica, v. 25, p. 164–171 (in Chinese with English abstract).

Zhou, X. M., 2003, My thinking about granite geneses of South China: Geological Journal of China Universities, v. 9, p. 556–565 (in Chinese with English abstract).

Zhou, X. M., and Li, W. X., 2000, Origin of late Mesozoic igneous rock in SE China: Implications for lithosphere subduction and underplating of mafic magmas: Tectonophysics, v. 326, p. 269–287.

Zhu, B. Q., Wang, H. F., Chen, Y. W., Chang, X.-Y., Hu, Y.-G.,and Cie, J., 2004, Geochronological and geochemical constraint on the Cenozoic extension of Cathaysian lithosphere and tectonic evolution of the border sea basins in East Asia: Journal of Asian Earth Science, v. 24, p. 163–175.

Zindler, A., and Hart, S. R., 1986, Chemical geodynamics: Annual Review of Earth and Planetary Sciences, v. 14, p. 493–571.

Zou, H. B., Zindler, A., Xu, X. S., and Qi, Q., 2000, Major, trace element, and Nd, Sr, and Pb isotope studies of Cenozoic basalts in SE China: Mantle sources, regional variations, and tectonic significance: Chemical Geology, v. 171, p. 33–47.

Zyabrev, S., and Matsuoka, A., 1999, Late Jurassic (Tithonian) radiolarians from a clastic unit of the Khabarovsk complex (Russian Far East): Significance for subduction accretion timing and terrane correlation: The Island Arc, v. 8, p. 30–37.